Part II

Interplay of Generic Interactions and Specific Binding

Chapter 4

Thermodynamics of polymer-tethered ligand-receptor interactions between surfaces

4.1 Introduction

Cells communicate via ligand-receptor interactions (Alberts et al., 2002; Baltimore et al., 2003). Such non-covalent interactions, which are present between specific pairs of residues in proteins or polypeptides, are specific (one-to-one) and reversible (Lauffenburger and Linderman, 1993). The interplay between specific and other generic physical interactions, such as electrostatic, hydrophobic and steric interactions (Israelachvili, 1992), is crucial to the adhesion and signalling between cells and the extracellular matrix, and has been extensively studied by researchers in physiology, biochemistry, biophysics, and bioengineering (Alberts et al., 2002; Bongrand, 1999; Hammer and Tirrell, 1996; Orsello et al., 2001; Zhu et al., 2000; Baudry et al., 2004; Cuvelier et al., 2004). Understanding specific cellular interactions, especially their interplay with other generic interactions in biological processes, assists bioengineering design, such as tissue engineering and bio-specific recognition. On the other hand, artificially-designed bio-mimetic materials, such as polymersomes (Discher et al., 1999; Lin et al., 2004; Bermúdez et al., 2004; Lin et al., 2005), vesicles or liposomes (Cuvelier et al., 2004; Cuvelier and Nassoy, 2004), and substrate-supported monolayer and bilayer membranes (Sackmann, 1996; Tanaka and Sackmann, 2005) allow better characterization of the specific and non-specific interactions because of the absence of complicating factors such as chemical signaling and deformability of biological cells *in vivo* (Lawrence and Springer, 1991; Dustin et al., 1996; Finger et al., 1996; Kuo and Lauffenburger, 1993; Eniola et al., 2003).

Designing biomaterials with biocompatibility requires qualitative understanding of the ligand-receptor interactions. In the classical model of cell adhesion proposed by Bell, Dembo, and Bongrand (Bell, 1978; Bell et al., 1984; Torney et al., 1986; Dembo and Bell, 1987) (illustrated in Fig. 4.1), ligand-receptor binding is treated as a chemical equilibrium between ligand and receptor molecules, the interplay between specific binding and generic physical interactions resulting in an equilibrium constant dependent on the separation between the adhesion surfaces. The Bell model captures the qualitative features of cell adhesion and has been successful in fitting certain experimental measurements quantitatively. However, careful inspection of the theory reveals several flaws and confusions. First, the equilibrium constant in the Bell model is by definition for a chemical reaction in two dimensions (2D), which can only be inferred from measurements in bulk solutions (3D), but the relation between these two equilibrium constants is obscure and often causes confusion (Dustin et al., 1996; Orsello et al., 2001; Zhu et al., 2000). A rigorous treatment of the statistical thermodynamics of binding in a 2D system is still lacking. Second, a chemical-equilibrium treatment implicitly assumes that the ligand and receptor molecules are mobile on the surfaces, which is valid only when molecules are embedded in a fluid bilayer or membrane. In many experimental settings ligands and receptors are fixed on beads (Kuo and Lauffenburger, 1993; Eniola et al., 2003) or covalently linked (Lin et al., 2004; Bermúdez et al., 2004), therefore the chemical-equilibrium assumption fails (Martin et al.,

2006) and it is erroneous to extract the parameters of the Bell model from these measurements by fitting to a chemical equilibrium expression naively.

In many biological or engineering systems, ligand or receptor groups are tethered by polymers or polypeptides to enhance specificity (Garcia, 2006; Chen and Dormidontova, 2005) or achieve different functions (Springer, 1990, 1994). Polymer-tethering has also been a common motif in surface force measurements and single-molecule studies (Wong et al., 1997; Jeppesen et al., 2001). The polymer tether turns the short-range lock-and-key type interaction into a long-range specific interaction, which has important implications to the equilibrium as well as dynamic properties of adhesion (Martin et al., 2006; Moore and Kuhl, 2006; Moreira and Marques, 2004; Sain and Wortis, 2004), and suggests a new route to controlling the interactions between surfaces typically achieved by generic physical interactions (Israelachvili, 1992; Hiddessen et al., 2000; Carignano and Szleifer, 2003; Nap and Szleifer, 2005). To characterize the polymer-tethered ligand-receptor binding, we need to separate the contributions to the effective binding constant from molecular binding and from conformation degrees of freedom—a single phenomenological binding constant is inadequate.

In this paper we study a microscopic model of polymer-tethered ligand-receptor binding and analyze the thermodynamics of binding as well as the interactions between surfaces mediated by the ligands and receptors. We explicitly account for the degrees of freedom of the flexible polymer tether, and separate their contributions to the effective binding affinity as measured in experiments. Specific attention is paid to the quenched case, where both ligands and receptors are immobile with random distributions. In this scenario the physical free energy is the average over the random distributions of ligands and receptors ("quenched average"), and an "effective binding constant" is not applicable. In the low-density regime, the quenched system has qualitatively different thermodynamics than the annealed system. We develop an asymptotic expansion of the quenched free energy of binding in terms of the scaled molecular densities of ligands and receptors, which extends our previous analysis for the single-ligand problem (Martin et al., 2006). The leading-order contributions (which are accurate at low densities and intermediate binding strength) allow us to derive the dependence of the binding free energy and the fraction of bound molecules on the microscopic binding affinity and the tether chain lengths, which are qualitatively different from the annealed systems.

Another feature of this paper is that we distinguish between ligands and receptors with fixed densities (closed) and connected to a reservoir with fixed chemical potential (open). In the Bell model the densities of ligands and receptors are both assumed to be the bulk average values. However, both experiments (Dustin et al., 1996) and theoretical estimations (Bruinsma et al., 2000; Bruinsma and Sackmann, 2002) suggest that in the adhesion of cells or vesicles, the small contact adhesion zones have ligand-receptor bonds aggregated at much higher densities than the bulk average. In this scenario the whole non-contact area serves as a reservoir for the small adhesion zones; therefore the adhesion part should be more naturally treated as an open system with a reservoir of molecules.

The biological implications are briefly discussed in Section 4.3.2. For further discussions in relation to experiments, see Bruinsma and Sackmann (2002).

We illustrate all our calculations using the ideal-Gaussian-chain model for the polymer tether and highlight the scaling dependences on the contour chain length (kuhn length); extensions to more complicated realistic models are straightforward (Szleifer and Carignano, 1996; Chen and Dormidontova, 2005). The Gaussian model allows exact analytical calculations of the chain confinement repulsion as well as the chain stretching energy, which are the main motifs in addition to the specific binding. We find that both at the onset of binding (where ligand-receptor pairs start to form) and at the free energy minimum (bridging conformation is most stable), the surface separations scale linearly as the spatial extension of the Gaussian chain. While the equilibrium separation is found to be insensitive to the binding energy, the onset of binding is proportional to the square root of the binding energy $\sqrt{\epsilon/k_{\mathrm{B}}T}$ as was suggested by Moore and Kuhl (2006). These result in a quasi-equilibrium critical tension for breaking a tethered ligand-receptor bond that scales as $N^{-1/2}$.

This chapter extends our previous paper (Martin et al., 2006) where a discrete lattice model was used and adhesion was between a single ligand and receptors. In Section 4.2 we define the continuum model for tethered ligand-receptor binding as illustrated in Fig. 4.1, and present the theoretical analysis. For simplicity we choose to study univalent ligands and receptors with monodisperse tether lengths. In Section 4.3 we discuss the key features for the simple system corresponding to the model solved in Section 4.2, and go on to study several examples combining different types of specific and non-specific interactions based on the results in Section 4.2. We suggest some tentative guidelines for the control over the interactions between surfaces via specific binding. The main conclusions are summarized in Section 4.4 with brief discussions on relevant problems.

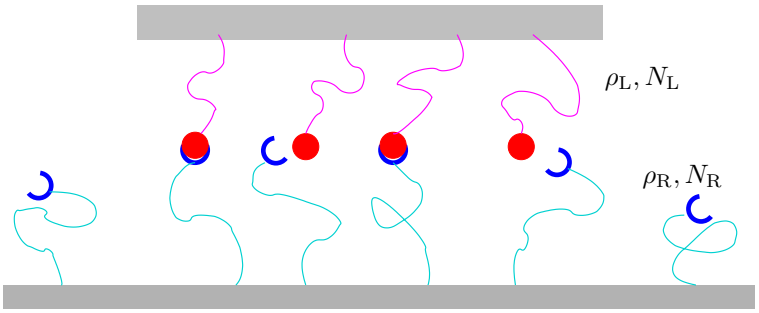

Figure 4.1: Schematic view of the model for surfaces with tethered ligands and receptors. The surfaces are separated by a distance L_z, the polymer tethers have mean square end-to-end distance $N_{\mathrm{L}}b^2$ and $N_{\mathrm{R}}b^2$, with area densities ρ_{L} and ρ_{R} for ligands and receptors, respectively; the anchoring ends are located within distance z_0 from the surface. In the Bell model, binding between ligands and receptors is treated as a chemical equilibrium with constant K dependent on the surface separation. Here we assume the binding between a ligand residue and a receptor residue to have an equilibrium constant K_0 as can be measured in a bulk solution of proteins.

4.2 Model and solution

The model is schematically shown in Fig. 4.1. Definitions of variables are given in Table. 4.1. We assume the anchoring ends on the surfaces to be non-interacting (i.e., ideal gas in 2D), and the surfaces are non-adsorbing and impenetrable for the polymer segments.

The binding (ligand and receptor) groups are located at the free ends of the polymers. The binding affinity is characterized by the equilibrium constant K_0 of the reaction

$$L + R \rightleftharpoons LR$$

in a bulk solution of ligand and receptor proteins (without the polymer tether), as is given by

$$K_0 = \frac{c_{\rm LR}}{c_{\rm L} c_{\rm R}}.$$

In our calculations all densities are molecular densities instead of molar densities.

From statistical thermodynamics we know that

$$K_0 = \frac{q'_{\rm LR}}{q'_{\rm L} q'_{\rm R}},$$

where $q'_{\rm i} = q_{\rm i}/V$ (i = L, R, or LR) is the internal part of the partition function for species i. If molecules are tethered or confined, the translation part is modified, but we can assume that the internal partition function remains the same, i.e., $q'_{\rm i}$ is unaffected by the tether. For the current model as illustrated in Fig. 4.1, the equilibrium constant in terms of the surface densities of molecules is given by

$$K = \frac{\rho_{\rm LR}}{\rho_{\rm L}\rho_{\rm R}} = \frac{q_{\rm LR}/A}{q_{\rm L}/A \cdot q_{\rm R}/A} = \frac{q'_{\rm LR}}{q'_{\rm L} q'_{\rm R}} \cdot \frac{A q^{\rm t}_{\rm LR}}{q^{\rm t}_{\rm L} q^{\rm t}_{\rm R}} = K_0 \frac{A q^{\rm t}_{\rm LR}}{q^{\rm t}_{\rm L} q^{\rm t}_{\rm R}}. \tag{4.1}$$

$q^t_{\rm i}$ are the translation part of the partition function, which are calculated in Section 4.2.2.

Throughout the paper we use $c_{\rm i}$ to denote concentrations in 3D, in unit of "number of molecules per unit volume" and $\rho_{\rm i}$ for concentrations in 2D (number of molecules per unit area). Later on we also introduce a dimensionless density $\phi_{\rm i}$ which is $\rho_{\rm i}$ multiplied by the area spanned by the tether.

4.2.1 Thermodynamics of the surface interactions

Before discussing the thermodynamics of tethered binding, we first consider the general thermodynamics for the interactions between the surfaces with polymer-tethered ligands and receptors. The total free energy of interaction ΔF is measured by the free energy at given surface separation relative to infinite separation (non-interacting). Depending on the mobility and the relative fraction of the contact area to the whole surface, each species of molecules (ligands or receptors) can be in one of three different scenarios: immobile, mobile with a fixed density, or mobile with a fixed

Table 4.1: Glossary

Variable	Definition	Dimensions or Expressions
$N_{\rm i}b^2$	mean square end-to-end distance of the polymer tether	$[{\rm L}]^2$
$x_{\rm L}(x_{\rm R})$	fraction of tether lengths	$N_{\rm L}/(N_{\rm L}+N_{\rm R})$
$m_{\rm i}$	total number of molecules for each species	–
$c_{\rm i}$	number of molecules per unit volume	$[{\rm L}]^{-3}$
$\rho_{\rm i}$	number of molecules per unit area	$[{\rm L}]^{-2}$
$\phi_{\rm i}$	scaled density in 2D	$\rho_{\rm i}Nb^2$
$c_{\rm i}^{(0)}$, $\rho_{\rm i}^{(0)}$, $\phi_{\rm i}^{(0)}$	overall densities (both bound and unbound)	same as above
L	separation between surfaces	$[{\rm L}]$
l	scaled surface separation	$L/\sqrt{N}b$
$l_0(L_0)$	position of the free energy minimum	–
$l_1(L_1)$	onset of binding	–
$q_{\rm i}$	partition function of the tethered receptor	–
$q_{\rm i}'$	internal partition function	$[{\rm L}]^{-3}$
$q_{\rm i}^{\rm t}$	partition function of the polymer tether	$[{\rm L}]^3$
F	total free energy	$k_{\rm B}T$
ΔF	interaction free energy	$k_{\rm B}T$
$F_{\rm b}, F_{\rm r}$	contribution to ΔF from *binding* and *repulsive confinement*	$k_{\rm B}T$
$\mu_{\rm i}$	reservoir chemical potential	$k_{\rm B}T$
Ξ, Q	grand partition function for open systems	–
W, p	grand potential, osmotic pressure	$k_{\rm B}T$
K_0	standard binding constant in terms of $c_{\rm i}$	$[{\rm L}]^3$
K	2D binding constant in terms of $\rho_{\rm i}$	$[{\rm L}]^2$
$(\tilde{\epsilon})\epsilon$	(effective) binding energy	$k_{\rm B}T$
A	surface area	$[{\rm L}]^2$
$A_{\rm L}^{(0)}(A_{\rm R}^{(0)})$	total area of the surface occupied by ligands (receptors)	$[{\rm L}]^2$
$G(\mathbf{r},\mathbf{r}';N)$	Green's function of the polymer chain	$[{\rm L}]^{-3}$
z_0	anchoring distance	$[{\rm L}]$
$T(T_{\rm c})$	(critical) quasi-equilibrium tension force to break a single ligand-receptor bond	$[{\rm M}][{\rm L}]^{-1}[{\rm T}]^{-2}$
$\tau_{\rm D}$, $\tau_{\rm p}$, $\tau_{\rm r}$	different time scales	$[{\rm T}]$

chemical potential (connected to a reservoir). These different scenarios are described by different thermodynamic potentials.

For mobile receptors and ligands, the Helmholtz free energy can be written as

$$F_{\rm tot} = F_{\rm L}(A_{\rm L}^{(0)} - A, m_{\rm L}^{(0)} - m_{\rm L}) + F_{\rm R}(A_{\rm R}^{(0)} - A, m_{\rm R}^{(0)} - m_{\rm R}) + F(A, m_{\rm L}, m_{\rm R}).$$

Here $A_\alpha^{(0)}$ is the total area of the surface occupied by species α, $m_\alpha^{(0)}$ is the total number of molecules, A is the contact area, m_α is the number of molecules within the contact area A, F_α is the free energy of species α in the non-contact region on the surface, and F is the free energy in the contact region.

Before the surfaces are in contact, the free energy is

$$F_{\rm tot}^{(0)} = F_{\rm L}(A^{(0)}, m_{\rm L}^{(0)}) + F_{\rm R}(A_{\rm R}^{(0)}, m_{\rm R}^{(0)}).$$

Therefore the net interaction free energy is

$$\begin{aligned}\Delta F = {} & F(A, m_{\rm L}, m_{\rm R}) + F_{\rm L}(A_{\rm L}^{(0)} - A, m_{\rm L}^{(0)} - m_{\rm L}) - F_{\rm L}(A^{(0)}, m_{\rm L}^{(0)}) \\ & + F_{\rm R}(A_{\rm R}^{(0)} - A, m_{\rm R}^{(0)} - m_{\rm R}) - F_{\rm R}(A_{\rm R}^{(0)}, m_{\rm R}^{(0)}).\end{aligned} \tag{4.2}$$

If both species have fixed densities, we can take the surface in contact to be the entire surface, and $A_\alpha^{(0)} = A$. We have

$$\Delta F = F(A, m_{\rm L}, m_{\rm R}) - F_{\rm L}(A, m_{\rm L}) - F_{\rm R}(A, m_{\rm R}); \tag{4.3a}$$

If one species is connected to a reservoir with fixed chemical potential, then the total surface area for that species can be considered infinite relative to the contact area, e.g., $A_{\rm L}^{(0)} \gg A = A_{\rm R}$, then the net free energy of interaction is

$$\begin{aligned}\Delta F &= F(A, m_{\rm L}, m_{\rm R}) - F_{\rm R}(A_{\rm R}, m_{\rm R}) - A \left.\frac{\partial F_{\rm L}}{\partial A_{\rm L}}\right|_{A_{\rm L}=A_{\rm L}^{(0)}} - m_{\rm L} \left.\frac{\partial F_{\rm L}}{\partial m_{\rm L}}\right|_{m_{\rm L}=m_{\rm L}^{(0)}} \\ &= F(A, m_{\rm L}, m_{\rm R}) - m_{\rm L}\mu_{\rm L} - [F_{\rm R}(A, m_{\rm R}) - Ap_{\rm L}].\end{aligned} \tag{4.3b}$$

$p_{\rm L} = -\partial F_{\rm L}/\partial A_{\rm L}$ is the osmotic pressure of the ligands in the reservoir. For the case where both species are mobile, the interaction free energy is

$$\Delta F = F(A, m_{\rm L}, m_{\rm R}) - m_{\rm L}\mu_{\rm L} - m_{\rm R}\mu_{\rm R} + A(p_{\rm L} + p_{\rm R}) = -A(p - p_{\rm L} - p_{\rm R}). \tag{4.3c}$$

In these two cases the appropriate thermodynamic potential is given by $F - \mu_{\rm L} m_{\rm L}$ and $F - \mu_{\rm L} m_{\rm L} - \mu_{\rm R} m_{\rm R}$, respectively, corresponding to the case of open ensemble for ligands (closed ensemble for receptors), and open ensemble for both ligands and receptors.

If one species is immobile (localized) while the other is mobile, the immobile species essentially corresponds to the closed system with fixed densities. However, if both species are immobile, the translation degrees of freedom are lost. This case is referred to as the "quenched" case. Here we assume *a priori* that the quenched average free energy is self-averaging, i.e.,

$$\frac{1}{A} \lim_{A\to\infty} F(A) = \mathcal{F} = \Big\langle F(\{\mathbf{x}_{\rm i}\}, \{\mathbf{y}_{\rm j}\}) \Big\rangle,$$

A is the total surface area; the first equation defines the average free energy in the thermodynamic limit, and the second implies that this is equivalent to the average over different distributions of the quenched molecules.

In the quenched case the binding free energy is a random variable dependent on the distribution of molecules, and its average is essentially different from the annealed cases (where either of the

species is mobile). Let us first look at the simple case when ligands and receptors are put on a lattice with no tether, i.e., binding occurs only between molecules directly facing each other, then the quenched average of the binding free energy is just

$$\langle F_{\rm b}\rangle = -\rho_{\rm L}\rho_{\rm R}\epsilon,$$

where $\rho_{\rm L}$ and $\rho_{\rm R}$ give the probability of finding a ligand/receptor molecule within a unit area, and ϵ gives the energetic gain due to binding. Clearly this is different from the chemical equilibrium in the annealed cases.

Polymer tethers enlarge the range of binding between immobile ligands and receptors, as compared to the molecular case, nonetheless, at low densities most molecules are far apart: the physics of interactions is similar to the molecular case with a scaled density. In Section 4.2.3 we develop an asymptotic expansion in this low density limit for the binding free energy, from which the density (fraction) of bound pairs can be obtained.

In the rest of this subsection we discuss the relevant thermodynamic quantities for each of the annealed cases in detail; these results are quite general and do not depend on the specific model for the tether polymer; explicit treatment of polymer tethering will be described in detail in Section 4.2.2.

4.2.1.1 Both-open system

First we examine the system where both receptors and ligands are connected to a reservoir (in a grand canonical ensemble). The free energy of interaction is related to the grand canonical partition function, which is given by

$$\Xi(\mu_{\rm L},\mu_{\rm R}) = \exp\Big[e^{\beta\mu_{\rm L}}q_{\rm L} + e^{\beta\mu_{\rm R}}q_{\rm R} + e^{\beta(\mu_{\rm L}+\mu_{\rm R})}q_{\rm LR}\Big], \tag{4.4}$$

where $\mu_{\rm L}$ and $\mu_{\rm R}$ are the chemical potentials of ligands and receptors; $q_{\rm L}$, $q_{\rm R}$, and $q_{\rm LR}$ are the partition functions of ligands, receptors, and ligand-receptor pairs.

At equilibrium the chemical potential of the bound pair $\mu_{\rm LR}$ is equal to $\mu_{\rm L}+\mu_{\rm R}$, hence we can rewrite the above equation as

$$\Xi = \exp\Big(e^{\beta\mu_{\rm L}}q_{\rm L} + e^{\beta\mu_{\rm R}}q_{\rm R} + e^{\beta\mu_{\rm LR}}q_{\rm LR}\Big). \tag{4.4$'$}$$

And from the grand potential

$$W = -k_{\rm B}T\ln\Xi = -k_{\rm B}T\left(e^{\beta\mu_{\rm L}}q_{\rm L} + e^{\beta\mu_{\rm R}}q_{\rm R} + e^{\beta\mu_{\rm LR}}q_{\rm LR}\right), \tag{4.5}$$

we can obtain the 2D concentrations of ligands, receptors, and bound pairs in equilibrium

$$\rho_{\mathrm{i}} = \frac{1}{A}\frac{\partial \ln \Xi}{\partial \beta \mu_{\mathrm{i}}} = \frac{1}{A} e^{\beta \mu_{\mathrm{i}}} q_{\mathrm{i}} = \frac{q_{\mathrm{i}}^{\mathrm{t}}}{A} e^{\beta \mu_{\mathrm{i}}} q_{\mathrm{i}}' \quad (\mathrm{i} = \mathrm{L}, \mathrm{R}, \mathrm{LR}) \tag{4.6}$$

where $q_{\mathrm{i}}^{\mathrm{t}}$ is the translation part of the partition function. From these we obtain the relation between 2D and 3D binding constant as given by Eq. (4.1)

$$K = \frac{\rho_{\mathrm{LR}}}{\rho_{\mathrm{L}} \rho_{\mathrm{R}}} = K_0 \frac{A q_{\mathrm{LR}}^{\mathrm{t}}}{q_{\mathrm{L}}^{\mathrm{t}} q_{\mathrm{R}}^{\mathrm{t}}}.$$

In Eq. (4.6) $q_{\mathrm{i}}^{\mathrm{t}}$ depends on the surface separation L_z. At infinite separation ($L_z = \infty$) no binding occurs, therefore $\rho_\alpha(\infty)$ ($\alpha = \mathrm{L}, \mathrm{R}$) are just the reservoir concentrations $\rho_\alpha^{(0)}$,

$$\rho_\alpha^{(0)} = \frac{q_\alpha^{\mathrm{t}}(\infty)}{A} e^{\beta \mu_\alpha} q_\alpha'.$$

This relates ρ_{i} at finite surface separation L_z to the reservoir concentrations $\rho_\alpha^{(0)}$ as

$$\rho_\alpha = \rho_\alpha^{(0)} \frac{q_\alpha^{\mathrm{t}}(L_z)}{q_\alpha^{\mathrm{t}}(\infty)}, \qquad (\alpha = \mathrm{L}, \mathrm{R}) \tag{4.7}$$

$$\rho_{\mathrm{LR}} = K \rho_{\mathrm{L}}^{(0)} \rho_{\mathrm{R}}^{(0)} \frac{q_{\mathrm{L}}^{\mathrm{t}}(L_z) q_{\mathrm{R}}^{\mathrm{t}}(L_z)}{q_{\mathrm{L}}^{\mathrm{t}}(\infty) q_{\mathrm{R}}^{\mathrm{t}}(\infty)}. \tag{4.8}$$

The interacting free energy per unit area is given by the difference in the grand potential as given in Eq. (4.5)

$$\begin{aligned} \frac{\Delta F(L_z)}{A k_{\mathrm{B}} T} &= \frac{W(L_z)}{A k_{\mathrm{B}} T} - \frac{W(\infty)}{A k_{\mathrm{B}} T} \\ &= -\rho_{\mathrm{L}} - \rho_{\mathrm{R}} - \rho_{\mathrm{LR}} + \rho_{\mathrm{L}}^{(0)} + \rho_{\mathrm{R}}^{(0)} \\ &= \rho_{\mathrm{L}}^0 \left[1 - \frac{q_{\mathrm{L}}^{\mathrm{t}}(L_z)}{q_{\mathrm{L}}^{\mathrm{t}}(\infty)}\right] + \rho_{\mathrm{R}}^0 \left[1 - \frac{q_{\mathrm{R}}^{\mathrm{t}}(L_z)}{q_{\mathrm{R}}^{\mathrm{t}}(\infty)}\right] - K \rho_{\mathrm{L}}^0 \rho_{\mathrm{R}}^0 \cdot \frac{q_{\mathrm{L}}^{\mathrm{t}}(L_z)}{q_{\mathrm{L}}^{\mathrm{t}}(\infty)} \frac{q_{\mathrm{R}}^{\mathrm{t}}(L_z)}{q_{\mathrm{R}}^{\mathrm{t}}(\infty)}. \end{aligned} \tag{4.9}$$

4.2.1.2 Both-closed system

In the both-closed system the total number of molecules are fixed within the contact area. The chemical equilibrium between receptors, ligands, and bound pairs implies

$$K \left(\rho_{\mathrm{L}}^{(0)} - \rho_{\mathrm{LR}}\right) \left(\rho_{\mathrm{R}}^{(0)} - \rho_{\mathrm{LR}}\right) = \rho_{\mathrm{LR}},$$

which gives

$$\rho_{\mathrm{LR}} = \frac{1}{2}\left[\rho_{\mathrm{L}}^{(0)} + \rho_{\mathrm{R}}^{(0)} + K^{-1} - \sqrt{(\rho_{\mathrm{L}}^{(0)} + \rho_{\mathrm{R}}^{(0)} + K^{-1})^2 - 4\rho_{\mathrm{L}}^{(0)} \rho_{\mathrm{R}}^{(0)}}\right]. \tag{4.10}$$

Here $\rho_{\mathrm{LR}}, \rho_{\mathrm{L}}$, and ρ_{R} are 2D concentrations of ligand-receptor pairs, free ligands, and free receptors, and $\rho_\alpha^{(0)} = \rho_\alpha + \rho_{\mathrm{LR}}$ ($\alpha = \mathrm{L}, \mathrm{R}$) give the total concentration of ligands and receptors (both free and

bound) within the contact area.

The Helmholtz free energy is related to the grand potential by a Legendre transform[1]

$$\begin{aligned}\frac{F}{k_{\mathrm{B}}T} &= -\frac{W}{k_{\mathrm{B}}T} + \sum_{\alpha=\mathrm{L,R}} \frac{\mu_\alpha}{k_{\mathrm{B}}T}\left(\rho_\alpha + \rho_{\mathrm{LR}}\right) \\ &= -\rho_{\mathrm{L}} - \rho_{\mathrm{R}} - \rho_{\mathrm{LR}} + \sum_{\alpha=\mathrm{L,R}} \left(\rho_\alpha + \rho_{\mathrm{LR}}\right) \ln \frac{\rho_\alpha A}{q^{\mathrm{t}}_\alpha q'_\alpha}. \end{aligned} \tag{4.11}$$

The interaction free energy is given by

$$\begin{aligned}\frac{\Delta F(L_z)}{Ak_{\mathrm{B}}T} &= \frac{F(L_z)}{Ak_{\mathrm{B}}T} - \frac{F(\infty)}{Ak_{\mathrm{B}}T} \\ &= \rho_{\mathrm{LR}}(L_z) - \rho_L^{(0)} \ln \frac{q^{\mathrm{t}}_{\mathrm{L}}(L_z)}{q^{\mathrm{t}}_{\mathrm{L}}(\infty)} - \rho_{\mathrm{R}}^{(0)} \ln \frac{q^{\mathrm{t}}_{\mathrm{R}}(L_z)}{q^{\mathrm{t}}_{\mathrm{R}}(\infty)} + \rho_{\mathrm{L}}^{(0)} \ln \frac{\rho_{\mathrm{L}}(L_z)}{\rho_{\mathrm{L}}^{(0)}} + \rho_{\mathrm{R}}^{(0)} \ln \frac{\rho_{\mathrm{R}}(L_z)}{\rho_{\mathrm{R}}^{(0)}}. \end{aligned} \tag{4.12}$$

One can verify that if one species is immobile while the other is mobile and both have fixed number of molecules, the only difference is the translation entropy of the immobile species, which is independent of binding. Therefore the free energy of interaction is the same as in the both mobile case.

4.2.1.3 Open-closed system

Finally we examine the case in which one surface has a fixed number of molecules while molecules on the other has a fixed chemical potential. This corresponds to the scenario in which the two surfaces have different overall sizes, e.g., a virus binding to a cell, or a versicle or bead binding to a fluid bilayer.

Assuming that receptors have a fixed overall density, we have

$$\rho_{\mathrm{LR}} = K\rho_{\mathrm{L}}(\rho_{\mathrm{R}}^{(0)} - \rho_{\mathrm{LR}}) \Rightarrow \rho_{\mathrm{LR}} = \frac{K\rho_{\mathrm{R}}^{(0)}\rho_{\mathrm{L}}}{1 + K\rho_{\mathrm{L}}}, \tag{4.13}$$

which is simply the Langmuir isotherm for an ideal gas of ligands. ρ_{L} is related to the reservoir density as in Eq. (4.6)

$$\rho_{\mathrm{L}}(L_z) = \rho_{\mathrm{L}}^{(0)} \frac{q^{\mathrm{t}}_{\mathrm{L}}(L_z)}{q^{\mathrm{t}}_{\mathrm{L}}(\infty)}.$$

The thermodynamic potential of interest is obtained from the grand potential through a Legendre transform over the fixed density and the free energy of interaction is given by

$$\frac{\Delta F}{Ak_{\mathrm{B}}T} = \rho_{\mathrm{L}}^{(0)} - \rho_{\mathrm{L}}(L_z) + \rho_{\mathrm{R}}^{(0)} \ln \frac{\rho_{\mathrm{R}}(L_z)}{\rho_{\mathrm{R}}^{(0)}} - \rho_{\mathrm{R}}^{(0)} \ln \frac{q^{\mathrm{t}}_{\mathrm{R}}(L_z)}{q^{\mathrm{t}}_{\mathrm{R}}(\infty)}. \tag{4.14}$$

[1] Note that in Eq. (4.3a) m_α refer to the total number of ligands or species within the contact area, including both free molecules and bound ones; here ρ_{i} refer to the density of the free molecules only.

This also applies to the case in which receptors are immobile, where the difference due to the translational entropy is a constant independent of binding.

The results are summarized in Table. 4.2. In the next subsection we study the effects of the polymer tether and derive the expressions of q_i^t for the Gaussian chain model. The quenched case is treated separately in Section 4.2.3.

Table 4.2: Summary of different scenarios

	ligands	receptors	ensemble	expressions
I	immobile	immobile	quenched	(4.33), (4.36)
II	fixed c	fixed c	canonical ensemble	(4.3a), (4.10), (4.12)
	fixed c	immobile		
III	fixed μ	fixed c	open-closed	(4.3b), (4.13), (4.14)
	fixed μ	immobile		
IV	fixed μ	fixed μ	grand canonical	(4.3c),(4.8), (4.9)

4.2.2 Polymer-mediated specific interactions

In this subsection we calculate the contribution of polymer tethers to the ligand-receptor interactions. Before presenting the exact analytical calculations for the Gaussian chain, we first explore the scaling behavior of the physical quantities of interest.

4.2.2.1 Scaling analysis

As mentioned above, polymer tethers have two effects: chain stretching in binding, and repulsion between the surfaces due to short-range confinement. Both effects are classic problems in polymer physics (de Gennes, 1979). A systematic scaling analysis of polymers confined between surfaces can be found in Lipowsky (1995), and Manghi and Aubouy (2003). Here we analyze the scaling of the size of the polymer tether in the presence of ligand-receptor binding. The scaling analysis is carried out for a polymer chain with Flory exponent ν, (i.e., $< R^2 > \sim N^{2\nu} b$). The Gaussian chain results follow by take $\nu = 1/2$.

When surfaces are far apart, the polymer chain is confined in a semi-infinite space, which gives the reference state for the problem. As surfaces come closer, ligand and the receptor groups at chain ends can meet and bind with each other. We assume that at this stage the two surfaces are still far apart so that the polymer chain is significantly stretched and chain confinement can be neglected, which will be justified *a posteriori*. In the strong stretching regime, the polymer chain can be viewed as a string of blobs of size ξ. Then the stretching energy is given by

$$E \sim k_B T \times \text{number of blobs} \sim \frac{N}{(\xi/b)^{1/\nu}},$$

and the equilibrium end-to-end distance is

$$L_z \sim N\xi^{1-\frac{1}{\nu}} b^{1/\nu}.$$

Therefore the stretching energy is given in terms of the end-to-end distance as

$$\frac{E}{k_{\mathrm{B}}T} \sim N\left(\frac{L_z}{Nb}\right)^{\frac{1}{1-\nu}} = \left(\frac{L_z}{N^{\nu}b}\right)^{\frac{1}{1-\nu}}. \tag{4.15}$$

When binding becomes possible, the molecular binding energy ϵ becomes comparable to the stretching energy, hence we have for the separation L_z^1 corresponding to the onset of binding

$$\left(\frac{L_z^1}{N^{\nu}b}\right)^{\frac{1}{1-\nu}} \sim \frac{\epsilon}{k_{\mathrm{B}}T} \Rightarrow L_z^1 \sim (\epsilon/k_{\mathrm{B}}T)^{1-\nu} N^{\nu} b. \tag{4.16}$$

This justifies our initial assumption that confinement is negligible in this regime.

As surfaces come very close, the polymer chains are squeezed by the surfaces into a string of blobs on a plane parallel to the surfaces, with thickness L_z. The blob size is

$$\xi \simeq L_z,$$

therefore free energy due to confinement is

$$V = k_{\mathrm{B}}T \frac{N}{(L_z/b)^{1/\nu}}. \tag{4.17}$$

Putting these two terms together with the binding energy, the overall free energy of a single ligand-receptor pair is (C_1 and C_2 are dimensionless constants)

$$\frac{F}{k_{\mathrm{B}}T} = -f\left[\frac{\epsilon}{k_{\mathrm{B}}T} - C_1\left(\frac{L_z}{N^{\nu}b}\right)^{\frac{1}{1-\nu}}\right] + C_2\frac{N}{(L_z/b)^{1/\nu}}, \tag{4.18}$$

and attains minimum at L_z^0 which is given by

$$L_z^0 \sim f^{-\nu(1-\nu)} N^{\nu} b, \tag{4.19}$$

where f is the fraction of ligand-receptor bridges per ligand-receptor pair. For $\epsilon \gg k_{\mathrm{B}}T$, $L_z^1 \gg N^{\nu}b$, hence binding overcomes stretching energy and most molecules are bound ($f \approx 1$), therefore the equilibrium separation between the surfaces is given by $L_z^0 \sim N^{\nu}b$.

The quenched case is more subtle. Assume $\epsilon \gg k_{\mathrm{B}}T$. The binding fraction of a tethered ligand is essentially the probability of finding a receptor within the "natural extension" of the ligand tether,

$\rho_{\mathrm{R}}\left\langle r_{\parallel}^2\right\rangle$. (Here "$\langle\rangle$" denotes the average over different chain conformations.) For a stretched chain, $r_{\parallel}^2$ is given by an ideal string of blobs in 2D,

$$\left\langle r_{\parallel}^2\right\rangle \simeq \frac{N}{(\xi/b)^{1/\nu}}\xi^2 \sim Nb^2\left(\frac{N}{L_z}\right)^{\frac{2\nu-1}{1-\nu}}, \tag{4.20a}$$

while for a confined chain the "natural" size of the tether parallel to the surface is that of a self-avoiding walk in 2D,

$$\left\langle r_{\parallel}^2\right\rangle \simeq \left[\frac{N}{(\xi/b)^{1/\nu}}\right]^{2\nu_2}\xi^2 \sim N^{2\nu_2}L_z^{2-2\nu_2/\nu}b^{2\nu_2/\nu}, \tag{4.20b}$$

ν_2 is the 2D Flory exponent.

For Gaussian chains, $\nu=\nu_2=1/2$, the scaling is the same in both cases, $f\sim Nb^2\rho_{\mathrm{R}}$, which is a scaled density of the receptor molecules. And we have (cf. Eq. (4.19))

$$L_z^0 \sim N^{1/2}b\left(\rho_{\mathrm{R}}Nb^2\right)^{-1/4}. \tag{4.21}$$

Hence we see that if ρ_{R} is kept constant $O(1)$, then the equilibrium occurs at a smaller surface separation compared to the annealed case. For swollen chains, $\nu\approx 3/5$ and $\nu_2=3/4$, the scaling in both scenarios (stretched and confined) also happen to be identical, and the probability for forming a ligand-receptor bridge is $f\sim\rho_{\mathrm{R}}N^{3/2}b^2(L_z/b)^{-1/2}$. The extra $L_z^{-1/2}$ factor suggests that as surfaces get closer, the polymer tether extends further in the direction parallel to the surface (since $\nu_2=3/4>\nu_3\approx 3/5$). The scaled density is given by $\rho_{\mathrm{R}}N^{3/2}b^2$, and the equilibrium separation is (cf. Eq. (4.19))

$$L_z^0 \sim bN^{15/22}\left(\rho_{\mathrm{R}}N^{3/2}b^2\right)^{-3/11} \sim N^{6/22}\rho_{\mathrm{R}}^{-3/11}. \tag{4.22}$$

Finally we can also estimate the interaction force between the surfaces due to binding. For a single bond, when the surfaces are pulled apart till the bond is broken, the total work done by the pulling force is roughly equal to the ϵ, hence we have (for binding fraction f) the average pulling force due to one ligand-receptor bond is

$$\tau \sim f\frac{\epsilon}{L_z^1-L_z^0} \sim \frac{fk_{\mathrm{B}}T}{N^{\nu}b}\left(\frac{\epsilon}{k_{\mathrm{B}}T}\right)^{\nu}. \tag{4.23}$$

4.2.2.2 Analytical calculations for the Gaussian chain

Here we carry out the exact analytical calculations for Gaussian chains. Since the internal partition functions q_{i}' is assumed to be unaffected by the polymer tether, all we need is the translation part of the partition function $q_{\mathrm{i}}^{\mathrm{t}}$ modified by the polymer tether. Using the Green's functions of the polymer

chain we can express $q_{\rm i}^{\rm t}$ as

$$q_{\rm LR}^{\rm t} = \int_{\mathbf{r}} \int_{\mathbf{r}_{\rm R},\mathbf{r}_{\rm L}} G(\mathbf{r},\mathbf{r}_{\rm R};N_{\rm R}) G(\mathbf{r},\mathbf{r}_{\rm L};N_{\rm L}) = \int_{\mathbf{r}_{\rm L},\mathbf{r}_{\rm R}} G(\mathbf{r}_{\rm L},\mathbf{r}_{\rm R};N_{\rm L}+N_{\rm R}); \tag{4.24a}$$

$$q_{\alpha}^{\rm t} = \int_{\mathbf{r}} \int_{\mathbf{r}_\alpha} G(\mathbf{r},\mathbf{r}_\alpha;N_\alpha) \qquad (\alpha = {\rm L},{\rm R}). \tag{4.24b}$$

Here $\mathbf{r}$ is the position of the ligand or receptor group in the space between the surfaces, and $\mathbf{r}_{\rm L}$ and $\mathbf{r}_{\rm R}$ are the positions of the anchoring ends of ligand or receptor tethers. Eq. (4.24) apply to any chain model for the polymer tether (as reflected in the Green's functions), as well as to both annealed and quenched cases: For annealed cases, $\mathbf{r}_{\rm L}$ ($\mathbf{r}_{\rm R}$) is restricted to the membrane whose integral is over a thin layer within distance z_0 from the surface; for the quenched case, it reduces to a summation over the positions of the immobile molecules.

For ideal Gaussian chain model, we can factorize the Green functions,

$$G(\mathbf{r}_1,\mathbf{r}_2;N) = g(\mathbf{u}_1,\mathbf{u}_2;N) h(z_1,z_2;N),$$

where $\mathbf{u}$ and z are the transverse (parallel to the surface) and the longitudinal (perpendicular to the surface) coordinates, and g and h are the transverse and the longitudinal part of the Green's functions. By translational invariance we have

$$g(\mathbf{u}_1,\mathbf{u}_2;N) = g(\mathbf{u}_1-\mathbf{u}_2;N),$$

and

$$\int_{\mathbf{u}_1,\mathbf{u}_2} g(\mathbf{u}_1,\mathbf{u}_2;N) = A \int_{\mathbf{u}} g(\mathbf{u};N).$$

For the end-anchored polymer chain we further assume that $z_0 \ll \sqrt{N}b$, and

$$\int_0^{z_0} dz h(z,z_1;N) \approx z_0 h(z_0,z_1;N) = z_0 h_0(z_1;N).$$

For small enough z_0, its value does not affect the physical quantities of interest, such as the binding constant or the free energy of interactions.

From Eq. (4.1), the binding constant is given by

$$K = K_0 \frac{A q_{\rm LR}^{\rm t}}{q_{\rm L}^{\rm t} q_{\rm R}^{\rm t}} = K_0 \frac{h_0(L_z;N_{\rm L}+N_{\rm R}) \int_{\mathbf{u}} g(\mathbf{u};N_{\rm L}+N_{\rm R})}{\int_{\mathbf{u}} g(\mathbf{u};N_{\rm L}) \int_z h_0(z;N_{\rm L}) \int_{\mathbf{u}} g(\mathbf{u};N_{\rm R}) \int_z h_0(z;N_{\rm R})}. \tag{4.25}$$

For Gaussian chains, $g(\mathbf{u})$ is a Gaussian distribution and the integration over $\mathbf{u}$ yields unity. We are left with

$$K = K_0 \frac{h_0(L_z;N_{\rm L}+N_{\rm R})}{\int_z h_0(z;N_{\rm L}) \int_z h_0(z;N_{\rm R})}. \tag{4.26}$$

The one-dimensional Green's function h_0 for a Gaussian chain confined between surfaces can be analytically solved; details are given in Appendix 4.A.

To highlight the scalings for Gaussian chains, it is convenient to rescale lengths by $\sqrt{N}b$, which is the mean square end-to-end distance. Here we choose to scale all lengths by $\sqrt{N_\mathrm{L}+N_\mathrm{R}}b = \sqrt{N}b$. (As is shown in Appendix 4.A, h_0 scales as a function of $L_z/\sqrt{N}b$.) With this rescaling the (dimensionless) receptor/ligand densities are given by

$$\phi_\alpha = \rho_\alpha N b^2, \tag{4.27}$$

with a dimensionless binding constant

$$\begin{aligned}\frac{\phi_\mathrm{LR}}{\phi_\mathrm{L}\phi_\mathrm{R}} &= \frac{K_0}{Nb^2}\frac{h_0(L_z/\sqrt{N}b)}{\int_z h_0(z/\sqrt{N_\mathrm{L}}b)\int_z h_0(z/\sqrt{N_\mathrm{R}}b)} \\ &= \frac{K_0}{(Nb^2)^{3/2}}\cdot\frac{\sqrt{N}bh_0(l)}{q^\mathrm{t}_\mathrm{L}(l)q^\mathrm{t}_\mathrm{R}(l)}.\end{aligned} \tag{4.28}$$

(Note that h_0 is of dimension [length]$^{-1}$, hence the second factor, which depends on the scaled surface separation $l = L_z/\sqrt{N}b$, is dimensionless.)

In the literature the dissociation constant K_d is frequently reported in unit of M (mol/litre) and a binding energy ϵ_0 is defined as

$$\epsilon_0 = -k_\mathrm{B}T\ln(K_\mathrm{d}/[\mathrm{M}]),$$

which is considered the binding energy measuring the intrinsic binding affinity. For most bound pairs ϵ_0 is found to be 5 to 30 $k_\mathrm{B}T$ (Moore and Kuhl, 2006). In our problem K_0 is given in terms of molecular densities, it is related to K_d as

$$K_0 = K_\mathrm{d}^{-1}N_\mathrm{a}^{-1},$$

where N_a is Avogadro's number.

Eq. (4.28) suggests that for tethered binding, we can define an effective binding energy

$$\ln\frac{\phi_\mathrm{LR}}{\phi_\mathrm{L}\phi_\mathrm{R}} = \frac{\tilde{\epsilon}(l)}{k_\mathrm{B}T} = \frac{\epsilon+\Delta\epsilon(l)}{k_\mathrm{B}T}, \tag{4.29}$$

$$\epsilon = k_\mathrm{B}T\ln\frac{K_0}{(Nb^2)^{3/2}}, \tag{4.30}$$

$$\Delta\epsilon(l) = k_\mathrm{B}T\ln\frac{\sqrt{N}bh_0(l)}{q_\mathrm{L}(l)q_\mathrm{R}(l)}. \tag{4.31}$$

$\Delta\epsilon(l)$ measures the energetic cost due to stretching of the polymer tether; while ϵ accounts for the

binding affinity excluding chain stretching. ϵ is related to ϵ_0 as

$$\epsilon = \epsilon_0 + \ln \frac{10^{-3}\mathrm{m}^3}{(Nb^2)^{3/2}N_\mathrm{a}}. \tag{4.32}$$

For tether lengths in the normal range $Nb \sim 10$nm while $b \sim 0.1$nm, the second term is of order 0.1. One can use either ϵ_0 or ϵ as a measure of the binding affinity in the tethered case; we adopt ϵ for convenience in the discussion of different energetic contributions to the binding.

4.2.3 Immobile receptors and ligands: low-density limit

Since the quenched case (both receptors and ligands are immobile) is qualitatively different from the annealed case, we discuss it in detail in this subsection.

As mentioned above, in this case the physical quantities of interest are averaged over the quenched distributions of the molecules. We assume the quenched distribution is uniform for each molecule on the surface, namely the probability that a particular molecule is found at $\mathbf{r}$ satisfies

$$p(\mathbf{r}_\alpha = \mathbf{r}) = \frac{1}{A}\mathrm{d}^2\mathbf{r}.$$

For each species (ligand or receptor), we assume that the distribution of molecules correspond to a particular realization of the grand canonical distribution controlled by a chemical potential μ,[2] then the probability distribution of samples with given number of molecules n in an area A is given by

$$p(n) = \frac{1}{Q}\frac{\lambda^n q^n}{n!},$$

where $\lambda = e^{\beta\mu}$ and the normalization (grand partition function) is

$$Q = \sum_n \frac{\lambda^n q^n}{n!} = \exp(\lambda q).$$

Hence for the ligand-receptor system, the quenched average free energy is given by

$$\bar{F} = \sum_{m_\mathrm{L}, m_\mathrm{R}} p(m_\mathrm{L}) p(m_\mathrm{R}) \left\langle F(m_\mathrm{L}, m_\mathrm{R}) \right\rangle. \tag{4.33}$$

The chemical potential is related to the (thermodynamic average) number density of molecules as

$$\rho_\alpha^{(0)} = \frac{1}{A}\frac{\partial \ln Q}{\partial \mu_\alpha} = \frac{\lambda_\alpha q_\alpha}{A}. \tag{4.34}$$

[2]Here we temporarily omit the subscript α for convenience.

Putting this back into Eq. (4.33) we have

$$\begin{aligned}\bar{F} &= \frac{1}{e^{A\rho_{\rm L}^{(0)}+A\rho_{\rm R}^{(0)}}}\sum_{m_{\rm L},m_{\rm R}}\frac{(A\rho_{\rm L}^{(0)})^{m_{\rm L}}(A\rho_{\rm R}^{(0)})^{m_{\rm R}}}{m_{\rm L}!m_{\rm R}!}\left\langle F(m_{\rm L},m_{\rm R})\right\rangle \\ &= A\left[\mathcal{F}^{(1,1)}\rho_{\rm L}^{(0)}\rho_{\rm R}^{(0)}+\mathcal{F}^{(1,2)}\rho_{\rm L}^{(0)}{\rho_{\rm R}^{(0)}}^2+\mathcal{F}^{(2,1)}{\rho_{\rm L}^{(0)}}^2\rho_{\rm R}^{(0)}+\cdots\right].\end{aligned} \tag{4.35}$$

(Note that we have reserved $\bar{F}$ for the "grand canonical average" and $\langle F(m_{\rm L},m_{\rm R})\rangle$ can be regarded as the "canonical average" free energy with given number of molecules, $m_{\rm L}$ and $m_{\rm R}$. It is easy to see that the largest term in the series in Eq. (4.35) has $m_{\rm L}=A\rho_{\rm L}^{(0)}$ and $m_{\rm R}=A\rho_{\rm R}^{(0)}$, therefore in the thermodynamic limit, the canonical average $< F >$ should be equal to the grand canonical average $\bar{F}$.) In Appendix 4.B we present the calculations for $\mathcal{F}^{(n,m)}$ up to $n=2,m=2$. The binding fraction is most conveniently obtained by taking the derivative of F with respect to $\beta\epsilon$ (or $\ln K$).

Despite that the expansion is asymptotic, the leading-order results are usually qualitatively accurate well beyond the range of densities in which the series is convergent, and here we present the results

$$\bar{F}=\bar{F}_{\rm b}(\text{binding})+F_{\rm r}(\text{repulsion})$$

$$\bar{F}_{\rm b}=-A\rho_{\rm L}^{(0)}\rho_{\rm R}^{(0)}\int_{\mathbf{u}}\ln\left\{1+\frac{3}{2\pi}\exp\left[\beta\tilde{\epsilon}(l)-\frac{3u^2}{2Nb^2}\right]\right\}, \tag{4.36a}$$

$$F_{\rm r}=-Ak_{\rm B}T\left[\rho_{\rm L}^{(0)}\ln\frac{q_{\rm L}^{\rm t}(L_z)}{q_{\rm L}^{\rm t}(\infty)}+\rho_{\rm R}^{(0)}\ln\frac{q_{\rm R}^{\rm t}(L_z)}{q_{\rm R}^{\rm t}(\infty)}\right], \tag{4.36b}$$

$$\bar{\rho}_{\rm LR}=\frac{2\pi}{3}Nb^2\ln\left(1+\frac{3}{2\pi}e^{\beta\tilde{\epsilon}}\right)\rho_{\rm L}^{(0)}\rho_{\rm R}^{(0)}. \tag{4.36c}$$

4.3 Results and discussion

In this section we discuss the key features of binding between polymer-tethered ligands and receptors, and the overall interactions between surfaces mediated by these polymers. To focus on the key aspects of the problem without complications due to other interactions we assume the ideal-Gaussian-chain model. As discussed at the end of Section 4.2.2, after rescaling by the ideal end-to-end distance of the polymer tether, we obtain the dimensionless quantities as listed in Table 4.3 (cf. Table. 4.1 for definitions of the variables).

Table 4.3: Scaled variables

surface separation	$l=L_z/\sqrt{N}b$
densities	$\phi_{\rm i}=\rho_{\rm i}Nb^2$
binding affinity	$\epsilon=k_{\rm B}T\ln\left[K_0/(Nb^2)^{3/2}\right]$
tether fraction	$x_\alpha=N_\alpha/(N_{\rm L}+N_{\rm R})$, $(\alpha={\rm L},{\rm R})$

Before the discussion, it is informative to estimate the values of these parameters. The aver-

age number of ligand/receptor molecules is $10^5 \sim 10^7$ per cell, and the average area of a cell is $10^{-7} \sim 10^{-6}\text{cm}^2$: these give the average area densities of receptors/ligands $\rho \sim 10^{12}/\text{cm}^2$. The average tether length (contour length) of integrins and selectins on lymphocyte cells is of order 10nm (Springer, 1990), which is comparable to the estimation in the Bell papers (Bell, 1978; Bell et al., 1984; Torney et al., 1986). Assuming the monomer size b to be $\sim 10^{-8}$cm we find

$$\phi \sim 10^{12} \cdot 10^{-6} \cdot 10^{-8} = 10^{-2},$$

which gives the overall (dimensionless) density of molecules on the cell surface. In other cases (e.g., a cell adhering to a large surface) where the adhesion zone is an open system (a small part of the whole surface), we estimate that $\phi \sim O(1)$ within the focal zone, and $\phi \sim 0.001$ outside the contact area (the reservoir) due to depletion of ligands and receptors.

The binding constant K_0 can be obtained from the dissociation constant K_d. In Dustin et al. (1996) the dissociation constant was found to be $K_\text{d} = 6\mu M$, and the binding constant is $K_0 = (K_\text{d} N_\text{a})^{-1} \approx 10^{-16}\text{cm}^3$, which corresponds to a binding energy (in unit of $k_\text{B}T$)

$$\ln \frac{K_0}{(Nb^2)^{3/2}} \approx \ln 10^5 \approx 12$$

in our definition. Bell et al. (1984) estimated the 2D binding constant to be $K^{2\text{D}} \sim 10^{-8}\text{cm}^2$, which gives a binding energy

$$\frac{\epsilon}{k_\text{B}T} = \ln \frac{K^{2\text{D}}}{(Nb^2)} \approx \ln 10^6 \approx 14$$

in our definition. Moore and Kuhl (2006) compiled a list of experimentally measured physical parameters of ligand-receptor binding and it was quoted that the average binding energy ϵ_0 (cf. Eq. (4.32)) of all available ligand-receptor pairs is about $15k_\text{B}T$. The numerical values of ϵ_0 and ϵ are comparable; in our calculations we take ϵ to be $10k_\text{B}T$ or $15k_\text{B}T$.

In the discussions we proceed as follows. In Section 4.3.1 we study the effects of polymer tether on specific binding and non-specific repulsion. In particular we examine the dependence of binding on the tether fractions x_L and x_R. In Section 4.3.2, we discuss in detail the interactions between surfaces mediated by ligand-receptor binding. We consider the following cases for the receptors and ligands: I. Quenched (both ligands and receptors are immobile); II. "Both closed" (either ligands or receptors are mobile, but both with fixed densities); III. "Open-closed" (ligands are connected to a reservoir, and receptors have a fixed density (either mobile or immobile), or vice versa); IV. "Both open" (both ligands and receptors are connected to a reservoir). Hereafter we will refer to these different scenarios as "case I" to "case IV."

We focus on the free energy of interaction and the average number of bound pair per ligand/receptor ("binding fraction"). In particular we discuss features including the dependences

of the equilibrium separation and the minimum free energy on the binding energy and the molecular densities; scaling relations are tested by analytical calculations. In addition we also study the equilibrium force-extension curve between the surfaces. Finally in Section 4.3.3, we study several systems combining different types of specific and non-specific interactions, including ligand-receptor pairs with different tether lengths or binding affinities, and additional repelling polymers between surfaces.

4.3.1 Effects of the polymer tether on specific binding and non-specific interactions

From Eqs. (4.29) and (4.62) we see that the binding affinity in both quenched and annealed cases is measured by the separation-dependent effective binding energy

$$\frac{\tilde{\epsilon}(l)}{k_{\rm B}T} = \frac{\epsilon}{k_{\rm B}T} + \ln \frac{\sqrt{N}bh_0(l)}{q_{\rm L}^{\rm t}(l)q_{\rm R}^{\rm t}(l)}.$$

Since ϵ is only weakly dependent on the chain length (cf. Table. 4.3), the dependence in the binding affinity is primarily contained in the scaled surface separation $l = L_z/\sqrt{N}b$ in the second term. In Appendix 4.A.1 we have worked out the close-form expressions for the second term in the asymptotic limits of large and small separations

$$\frac{\tilde{\epsilon}(l) - \epsilon}{k_{\rm B}T} \simeq \begin{cases} \ln \dfrac{\pi^2}{8l} & (l \ll 1), \\ \ln \left[3\sqrt{6\pi} l^2 e^{-3l^2/2} \sqrt{x_{\rm L} x_{\rm R}}\right] & (l \gg 1). \end{cases} \tag{4.37}$$

The effective binding constant (for the annealed case) is given by

$$K = \frac{\rho_{\rm LR}}{\rho_{\rm L}\rho_{\rm R}} = Nb^2 e^{\beta\tilde{\epsilon}(l)},$$

and from Eqs. (4.37) this becomes

$$K \propto \begin{cases} \dfrac{K_0}{l\sqrt{N}b} = \dfrac{K_0}{L_z} & (l \ll 1), \\ \dfrac{K_0}{\sqrt{N}b} l^2 e^{-3l^2/2} & (l \gg 1). \end{cases} \tag{4.38}$$

Bell and co-workers (Bell, 1978; Bell et al., 1984; Torney et al., 1986) suggested that the 2D binding constant should be related to the 3D binding constant as

$$K = \frac{K_0}{L_z}.$$

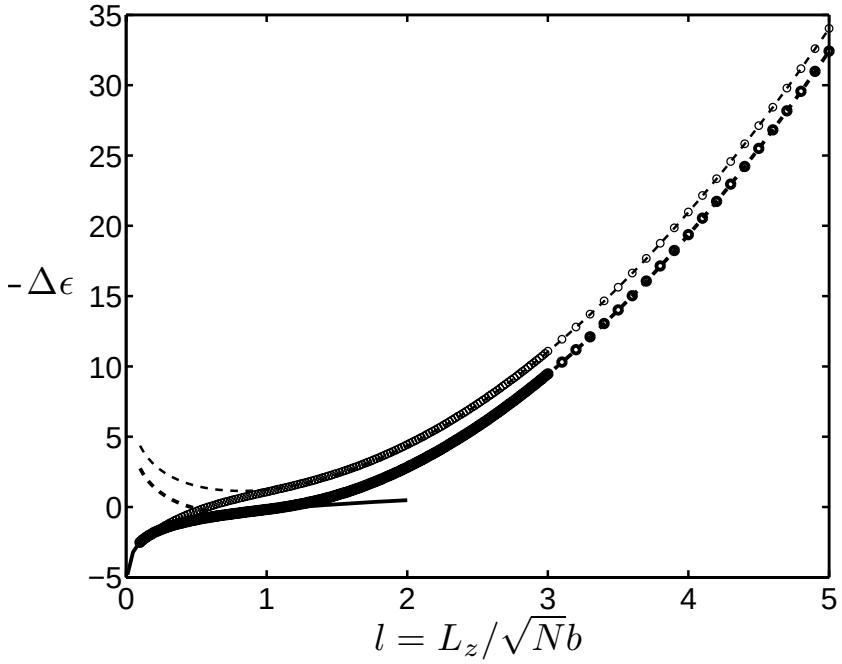

Figure 4.2: The contribution to the effective binding energy due to tether stretching: $-\Delta\epsilon = \epsilon - \tilde{\epsilon}(l)$. Here $-\Delta\epsilon$ is given in unit of $k_{\rm B}T$ and plotted against scaled surface separation $l = L_z/\sqrt{N}b$. Dash lines and the solid line are results from the asymptotic expressions in the limits $l \gg 1$ and $l \ll 1$, respectively; circles are from exact solutions. The thick dash line and circles are for equal tether lengths ($x_{\rm L} = x_{\rm R} = 0.5$), and the thin line and circles for a tether length ratio of $1 : 99$. In all calculations the total tether length $N = N_{\rm L} + N_{\rm R}$ is kept constant.

Our calculation establishes that this is valid only when surfaces are close enough, i.e., the surface separation is less than the ideal size of the tethered ligand-receptor bridge. When surfaces are far separate, the second expression implies a large stretching energy cost. Therefore one should be careful when inferring 2D binding constant from the 3D experimental data[3].

In Fig. 4.2 we plot $-\Delta\epsilon = \epsilon - \tilde{\epsilon}(l)$ in units of $k_{\rm B}T$ against the scaled surface separation $l = L_z/\sqrt{N}b$. (Here $-\Delta\epsilon$ can be interpreted as the free energy cost due to tether stretching.) We choose two different tether length ratios ($x_{\rm L}$): the thick lines and circles represent the case with equal tether lengths, $x_{\rm L} = x_{\rm R} = 0.5$; while the thin lines and circles are for the case with $x_{\rm L} = 0.01$ (equivalent to $x_{\rm R} = 0.01$ by symmetry). Here the circles represent results from exact solutions, dash lines are from the approximate expressions for large separations and the solid line is for small separations (in the latter case the results only depend on the total tether length and are identical in both cases).

For the whole range of surface separations the approximate expressions work remarkably well. In particular, the stretching energy cost is given by $3l^2/2$ to the leading-order, as was given by scaling

[3]In real situations the polymer tethers are probably not Gaussian, however, our scaling analysis (cf. Section 4.2.2.1) showed that the stretching regime and the confinement regime are qualitatively different, therefore it is impossible to have one expression valid for these different regimes.

arguments (de Gennes, 1979). We can define the onset of binding l_1 as where $\tilde{\epsilon} \gtrsim 0$, whence the density of bound pairs starts to increase significantly. Assuming that at l_1 the polymer tether is stretched, we can estimate l_1 as (from the asymptotic expression in the strong stretching limit)

$$l_1 = \frac{L_z}{\sqrt{N}b} \sim \sqrt{\epsilon/k_{\rm B}T} > 1, \tag{4.39}$$

which justifies our assumption *a posteriori*. Therefore for $\epsilon \gg k_{\rm B}T$, the tether chains are considerably stretched when ligand-receptor bridges start to form.

From Fig. 4.2 we also see that with total tether length $N = N_{\rm L} + N_{\rm R}$ fixed, binding is optimal if ligand and receptor tether lengths are equal; the difference between different tether ratios vanishes at small surface separations as can be inferred from Eq. (4.37). The $3k_{\rm B}T$ difference is purely an entropic effect, and allows the fine tuning of the binding affinity at intermediate or large surface separations without affecting the short-range behavior. This feature is especially relevant near the onset of binding, where $\tilde{\epsilon} \approx 0$, and a small difference in $\Delta\epsilon$ can result in a large change in l_1.

Another contribution from the polymers is the repulsion between surfaces due to the confinement of polymer segments. Figure 4.3 shows the dependence of the repulsive free energy on the surface separation for a single polymer with ideal end-to-end distance Nb^2.

From Appendix 4.A.1 we have obtained[4]

$$\frac{F_{\rm r}}{k_{\rm B}T} \simeq \begin{cases} -\ln\dfrac{4z_0}{l\sqrt{N}b} + \dfrac{\pi^2}{6l^2} & l \ll 1, \\ \\ -\ln\dfrac{4z_0}{\sqrt{N}b} - \ln\dfrac{\sqrt{6}}{4\sqrt{\pi}} & l \gg 1. \end{cases} \tag{4.40}$$

The constant in the limit $l \gg 1$ gives the free energy of confining a single Gaussian chain in half space, while the result for $l \ll 1$ scales as $1/l^2$, as is inferred from scaling arguments.

While the stretching energy cost flattens off at small surface separations, the repulsive free energy ($\sim 1/l^2$) increases sharply and dominates over the binding energy. On the other hand the stretching energy grows as l^2 at large separations and prohibits binding at large l. The net effect results in a total free energy minimum attained around $l = 1$, with low stretching energy and not too strong repulsion due to confinement. Next we discuss the total interaction due to tethered binding in different physical scenarios.

[4]In Fig. 4.3 we have substracted out the first term in Eqs. (4.40) involving the anchoring distance z_0, which is a constant for given chain length.

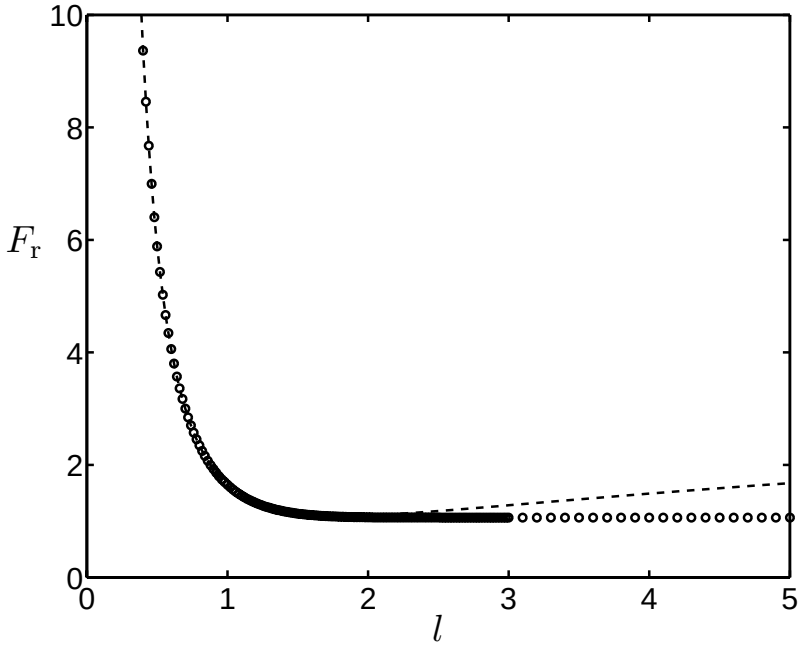

Figure 4.3: The free energy of confining a polymer between parallel surfaces. Circles are results from exact solutions and the dash line is from the asymptotic expression for $l \ll 1$.

4.3.2 Interactions between surfaces mediated by ligand-receptor binding

In this subsection we study 4 different scenarios according to the different mobilities of the species: case I (quenched), case II (both closed), case III (open-closed), and case IV (both open). The expressions for the density of bound molecules and the free energy of interactions are given by (cf. Table. 4.2) Eqs. (4.36) for the quenched case (case I), Eqs. (4.10) and (4.12) for the both-closed system (case II), Eqs. (4.13) and (4.14) for the open-closed system (case III), and Eqs. (4.8) and (4.9) for the both-open system (case IV).

While the quenched case applies to interacting surfaces with immobile molecules unambiguously, the different annealed cases can be difficult to distinguish. In particular we note that if one species is mobile, the thermodynamics is the same whether the other species with a fixed density are immobile or mobile. In reality a closed system (as in case II or case III) is best associated with surfaces with uniformly distributed molecules, such as lipid bilayers supported on flat substrates. An open system, on the other hand, corresponds to an inhomogeneous system with partial contact, such as flexible membranes or lipid bilayers supported on spherical particles. In these cases the non-contact part of the surface serves as a reservoir for the part in contact. Some typical examples of each cases are listed in Table. 4.3.2.

Here we focus on two quantities. The binding fraction f is defined as the number of bound

Table 4.4: Examples of different cases

Case I (quenched)	polymersomes, solid substrates, colloidal particles with attached polymers
Case II (both closed)	substrate-supporting lipid bilayers and monolayers
Case III (open-closed)	flexible membranes interacting with surfaces covered by immobile molecules
Case IV (both open)	flexible membranes, spherical vesicles

molecules divided by the number of molecules:

$$f = \frac{\rho_{\mathrm{LR}}}{\min(\rho_{\mathrm{L}}^{(0)}, \rho_{\mathrm{R}}^{(0)})};$$

the free energy per molecule is defined by

$$F(l) = \frac{\Delta F}{A \min(\rho_{\mathrm{L}}^{(0)}, \rho_{\mathrm{R}}^{(0)})},$$

which measures the strength of binding interactions between ligands and receptors. The definition of $F(l)$ coincides with the definition by Bell et al. (1984), and also allows a comparison with the single-chain calculation in our previous paper (Martin et al., 2006). To avoid ambiguity we choose $\rho_{\mathrm{L}}^{(0)} = \rho_{\mathrm{R}}^{(0)} = \rho$ ($\phi_{\mathrm{L}}^{(0)} = \phi_{\mathrm{R}}^{(0)} = \phi^{(0)}$) in our calculations. If both species are connected to a reservoir, then the density of bound pairs ρ_{LR} can be significantly higher than the reservoir densities $\rho_{\mathrm{L}}^{(0)}$ or $\rho_{\mathrm{R}}^{(0)}$; in this case f and F lose the meaning of "binding fraction" or "free energy per ligand or receptor," but purely serve as a comparison to the other cases (I, II, and III).

First we compare the different annealed cases (II, III, IV) where molecules are mobile. In Fig. 4.4, we show results for case II (thin lines) and case III (thick lines) with densities $\phi_{\mathrm{L}}^{(0)} = \phi_{\mathrm{R}}^{(0)} = 0.01$. The binding energy is taken to be $\epsilon = 10 k_{\mathrm{B}} T$ and equal tether lengths for ligands and receptors are assumed. We see that for $l \geq 0.5$, both cases are similar. In case III the binding fraction f saturates at a larger surface separation than in case II. In particular, near $l = 1$ the binding fraction is close to unity even for a lower reservoir density $\phi^{(0)} = 0.001$ (results not shown here). This indicates that molecules in the reservoir can be attracted into the system and bind with their counterparts; near the equilibrium bound state, the density of bound pairs is insensitive to the average density of ligands or receptors in the reservoir, but is determined from the binding constant and the (maximum) fixed density—this is consistent with the experimental observations by Dustin et al. (1996).

As surfaces come closer ($l < 1$), molecules start to feel the repulsion from the surfaces and are squeezed out from the contact area. At very small $l (< 0.5)$, the confinement repulsion dominates, and in case III even bound pairs are broken and molecules are pushed out into the reservoir; accordingly f drops to zero. In this regime of case III, the total interaction energy is the sum of the confinement free energy of the molecules remaining in the system and the osmotic pressure from the reservoir.

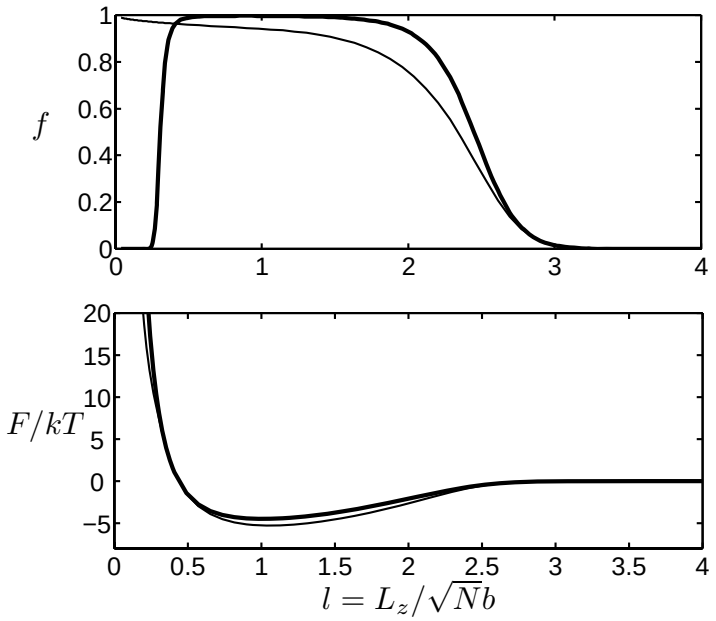

Figure 4.4: Comparison of case II ("both closed" system) and case III ("open-closed" system). The binding fraction f and the interaction free energy F are plotted against the scaled surface separation $l = L_z/\sqrt{N_{\rm L}+N_{\rm R}}b$. Thin solid lines are results for case II with $\phi^{(0)} = \rho_{\rm L}^{(0)}(N_{\rm L}+N_{\rm R})b^2 = 0.01$, ($\rho_{\rm L}^{(0)} = \rho_{\rm R}^{(0)}$); thick lines are for case III with the same densities. All calculations are for a binding energy $\epsilon = 10k_{\rm B}T$ and equal tether lengths.

We see that the free energy of interaction is always lower compared with case II due to the extra degrees of freedom of the species connected to a reservoir.

In Fig. 4.5 we compare case III ("open-closed") and case IV ("both open"). The binding energy is $\epsilon = 10k_{\rm B}T$, and all the densities are $\phi_{\rm L}^{(0)} = \phi_{\rm R}^{(0)} = 10^{-3}$. Here thin lines are for case III and thick lines for case IV; the dot line in Fig. 4.5(a) is the density of free (unbound) molecules with a reservoir. (From Eq. (4.13) if the reservoir densities are equal, the density of free molecules is the same in case III and case IV.) In both cases we see that as surfaces approach each other, free molecules are pushed out, while the densities of bound molecules hit a maximum near $l = 1$, close to the free energy minimum. But in the "both-open" system, we see a great enhancement of the local densities since both types of molecules can flow into the system due to binding attraction. As surfaces come even closer, both receptors and ligands are pushed out, the free energy in the "both open" system flattens off at $F = 2k_{\rm B}T$, which is the total osmotic pressure from the reservoir.

Next we compare the annealed case (case II) and the quenched case (case I) and discuss the features of binding in more detail.

Figure 4.6 shows F and f for case I (quenched) and case II (both closed) with scaled densities $\phi_{\rm L}^{(0)} = \phi_{\rm R}^{(0)} = 0.01$: the solid lines are results for case II; for the quenched case, the dash lines are results from the leading-order density expansion [$O(\phi_{\rm L}\phi_{\rm R})$], and circles are from expansions up to quartic order[$O(\phi^4)$]. To ensure accuracy of the density expansion, we choose a modest binding

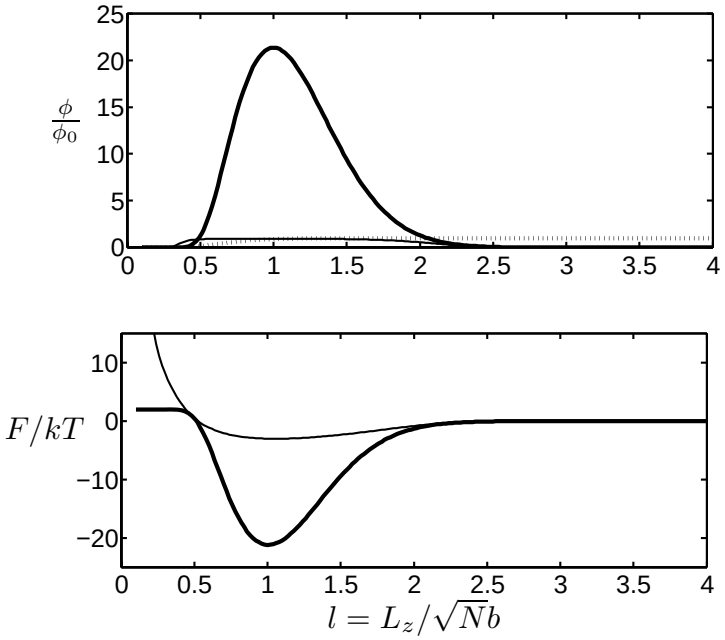

Figure 4.5: Comparison of case III ("open-closed") and case IV ("both open"). In either case all densities are chosen to be $\phi^{(0)} = 10^{-3}$. Upper figure shows densities of molecules relative to the reservoir density: the dot line represents the relative density of free molecules, thin and thick solid lines represent the relative densities of bound pairs for case III and case IV. Lower figure: Total free energy of interaction for case III (thin solid line) and case IV (thick solid line). The molecular binding energy is $\epsilon = 10k_{\rm B}T$.

energy $\epsilon = 10k_{\rm B}T$.

In both cases, we see that the binding fraction f starts to increase around $L_z/\sqrt{N}b = 3.5$, which corresponds to the onset of binding. At the onset of binding, very few bound ligand-receptor pairs are sparsely distributed and the situation is similar to isolated non-interacting ligand-receptor pairs, therefore the scaling dependence of l_1 on ϵ should be identical to that for a single ligand-receptor pair, $l_1 = L_z^1/\sqrt{N}b \sim \sqrt{\epsilon/k_{\rm B}T}$, as discussed previously. Indeed this scaling estimate gives $l_1 \approx 3.2$ for the Gaussian chain model, quite close to the exact results[5].

In the annealed case, as surfaces come closer, the binding fraction first increases rapidly and then gradually approaches unity, whence most molecules are bound. In the latter regime the separation between the surfaces is comparable to the size of the connected polymer tether, and ligand and receptor groups can reach anywhere between the surfaces with almost equal probability—put in other words, their densities are almost uniform in the space between the surfaces. This implies that the 2D binding constant K is related to the 3D constant K_0 as $K = K_0/L_z$. On the other hand, as surfaces come even closer the polymers start to feel stronger confinement from the surfaces, which contributes a repulsive free energy scaling as $1/l^2$ for Gaussian chains. The balance between

[5]Of course, for very strong binding $\beta\epsilon \gg 1$, we have $l_1 \gg 1$ and the Gaussian chain model becomes inaccurate. In this regime the finite extensibility of the polymer chain should be accounted for.

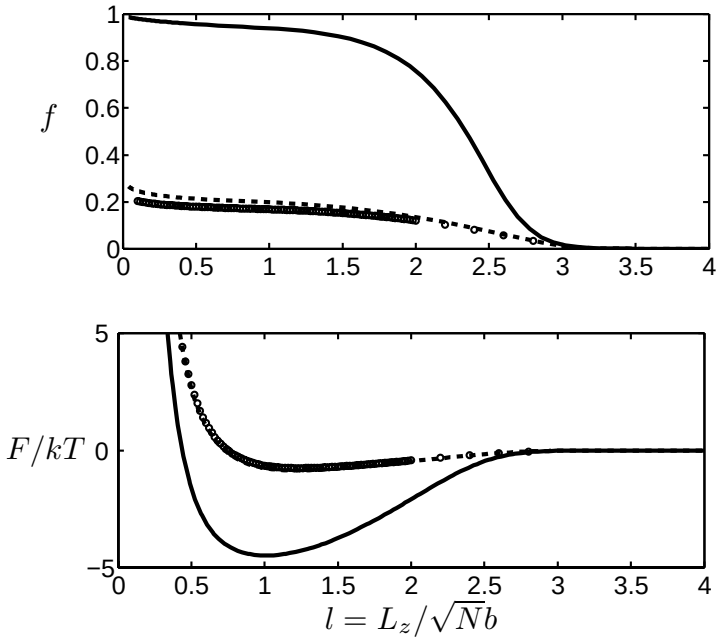

Figure 4.6: Comparison of case I ("quenched") and case II ("both closed"). Solid lines are for case II (mobile ligands and receptors with fixed densities), and dash lines are for case I (immobile ligands and receptors) from leading-order density expansion; Circles are results for the quenched case from second-order density expansion. The binding energy is $\epsilon = 10k_{\rm B}T$ and both ligands and receptors have a density $\phi^{(0)} = 0.01$.

the attractive binding and the repulsive confinement leads to a free energy minimum at $l_0 \approx 1$. Single-bound-pair scaling applies here as well because in this regime most molecules are bound, hence $f \approx 1$. For weaker binding such that the binding fraction has a substantial dependence on l, the equilibrium separation l_0 will also depend on ϵ, as will be discussed below.

We now investigate the quenched case. As discussed in Section 4.2.1, the free energy is averaged over the random distributions of the molecules. The generic repulsion due to confinement is independent of the relative positions of ligands and receptors; the quenched average is only invoked for the binding part. By the convexity of the free energy,

$$F_{\rm q} = -k_{\rm B}T\Big\langle \ln Q \Big\rangle \geq -k_{\rm B}T \ln\Big\langle Q \Big\rangle = F,$$

i.e., the quenched average is always larger than the annealed average. Hence the bound state in a quenched system has a higher free energy, and binding is less probable compared to the annealed case.

At least two factors contribute to the reduced tendency of binding between immobile molecules at low densities[6]. First, at low densities the anchoring ends of ligands and receptors are far apart, therefore the tether chains have to be laterally stretched for ligands and receptors to bind. This

[6]At high densities the quenched case should approach the annealed case.

lateral stretching adds an extra energetic cost to binding, and is only dependent on the densities and the tether lengths of the molecules. Another effect is due to the local inhomogeneity in molecule distributions[7]: due to fluctuations in the quenched distributions, locally there could be more ligands than receptors or vice versa, and the excess ones have no counterparts nearby, and remain unbound; while in the annealed case, these molecules can move around to locate their counterparts.

In the Gaussian chain model, the polymer chain is infinitely extensible. We can estimate the average number of molecules within an"accessible" distance as[8]

$$\rho R^2 = \rho N b^2 \epsilon / k_{\rm B}T = \phi\epsilon/k_{\rm B}T,$$

where the binding energy gain ϵ enables the tether to stretch farther to form a bridge. This gives an estimate for the maximal binding fraction, $f \lesssim \phi\epsilon/k_{\rm B}T$, which is attained when surfaces are very close. For reasonable values of ϵ with small ϕ it is always less than unity[9].

We also note that the asymptotic density expansion is accurate if the surface densities $\phi_{\rm L}, \phi_{\rm R}$ are small and binding energy is not too big. Since the density expansion is carried out around the no binding state, an empirical criterion is given by $\phi\epsilon/k_{\rm B}T < 1$, corresponding to the "weak" binding scenario. We see that the leading-order expansion is fairly accurate compared with the higher-order expansion (up to $O(\phi^4)$). Since we are mostly interested in the low-density regime when the quenched case and the annealed cases are most different, we shall use the leading-order result throughout the rest of the paper. From the leading-order expansion we have

$$\bar{\rho}_{\rm LR} \propto \rho_{\rm L}^{(0)} \rho_{\rm R}^{(0)} N b^2 \tilde{\epsilon},$$

this should be distinguished from the conventional binding equilibrium,

$$\rho_{\rm LR} \propto (\rho_{\rm L}^{(0)} - \rho_{\rm LR})(\rho_{\rm R}^{(0)} - \rho_{\rm LR}) e^{\beta\tilde{\epsilon}}.$$

In general there is no well-defined binding constant for the quenched case, especially when higher order terms $O(\phi^3)$ and $O(\phi^4)$ are relevant.

To summarize the binding favorability in different scenarios, we have

Both open $\gg$ open-close $\gtrsim$ both close $>$ quenched.

The difference is the entropic effect due to flexible polymers as well as to the diffusion of molecules in the reservoir. To better illustrate the difference between these cases, we plot in Fig. 4.7 the free

[7]This is briefly commented on by Moreira et al. (2003).

[8]When the surface separation is large, ϵ should be replaced by $\tilde{\epsilon}$ to account for the stretching energy.

[9]For finitely extensible chains, as in our previous paper (Martin et al., 2006), there is a strict upper bound set by the average number of molecules within the maximal extension in the limit of $\beta\epsilon \to \infty$, which is completely determined by the molecular density and maximal tether extension.

energy of binding and the binding fraction against the density of one species (receptors or ligands) while keeping the other fixed $\phi^{(0)} = 0.01$ (F and f is normalized to this fixed density). We see that for the quenched case the free energy and binding fraction increases almost linearly with the density, the slope is small, reflecting the restricted availability of binding molecules. In case II and case III where the maximum density of bound pairs is set by the fixed density of one species, as the density of the other species increases, f first increases exponentially but then approaches saturation. In case IV, the increase is linear all the way with a much larger slope that is proportional to K (cf. Eqs. (4.8) and (4.9)); this reflects a positive feedback effect: increasing the density of one species automatically attracts more molecules of the other species from the reservoir.

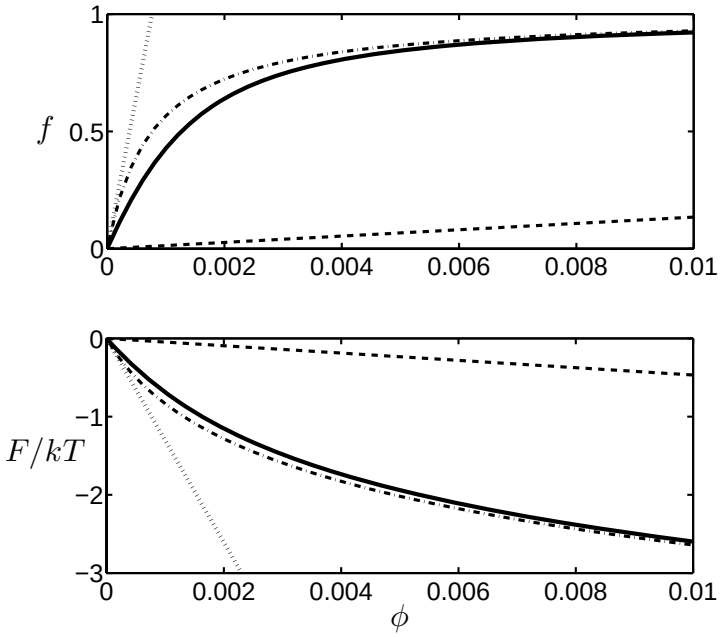

Figure 4.7: Dependence of the binding fraction and the free energy on the density of molecules for case I (dash line), II (solid line), III (dash dot line), and IV (dot line). The binding energy is $\epsilon = 10k_{\mathrm{B}}T$; receptors and ligands have equal tether lengths, one species has a fixed density $\phi^{(0)} = 0.01$, while the other has a varying density. The free energy and the binding fraction are calculated for a fixed surface separation $l = 1$ ($L_z = \sqrt{N}b$), which is near the equilibrium position (cf. Fig. 4.8).

Next we focus on the features related to the equilibrium separation l_0 and the equilibrium (minimum) free energy. From our scaling analysis in Section 4.2.2, for Gaussian chains the interaction free energy (per bound pair) can be written as

$$\frac{F}{k_{\mathrm{B}}T} \approx -f\left(\frac{\epsilon}{k_{\mathrm{B}}T} - C_1 l^2\right) + \frac{C_2}{l^2}.$$

The first term gives the total stretching and binding energy, while the second term measures the repulsion due to confinement. Assuming that f has a weaker dependence on l compared with the

stretching energy and the confinement repulsion[10], we obtain the equilibrium separation as

$$l^0 \approx f^{-1/4},$$

and the minimum free energy

$$\frac{F_{\min}}{k_{\rm B}T} \approx -f\frac{\epsilon}{k_{\rm B}T} + C_3 f^{1/2}.$$

The only dependence of l_0 on the binding energy is contained in f. From previous discussions we have seen that for reasonably large binding energy, f is close to unity near the equilibrium position in the annealed cases, therefore in these scenarios we expect l_0 to reach a constant if $\epsilon/k_{\rm B}T \gg 1$, this is indeed true as shown from in Fig. 4.8.

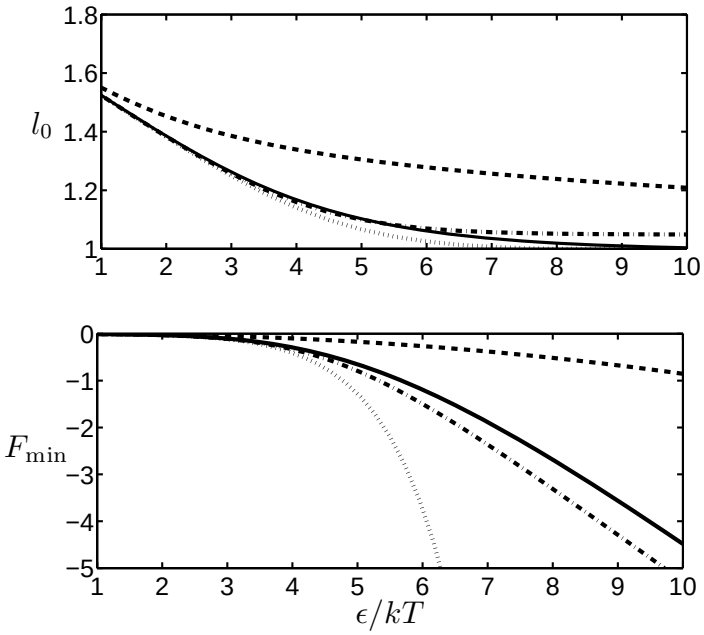

Figure 4.8: The dependence of the equilibrium separation and free energy on the molecular binding energy for case I (dash line), II (solid line), III (dash dot line), and IV (dot line). Ligands and receptors have equal tether length, with densities $\phi^{(0)} = 0.01$.

In Fig. 4.8 we plot l_0 and the equilibrium free energy for different binding energies. Broken lines represent the quenched case, solid lines for case II (both closed), dash-dot lines for case III (open-closed), and dot lines for case IV (both open). The receptors and ligands have equal tether lengths, with equal density $\phi_{\rm L}^{(0)} = \phi_{\rm R}^{(0)} = 0.01$. We observe that for the annealed cases in which the binding fractions reach unity in the strong binding regime, l_0 approaches 1, where the total energy due to stretching and confinement is minimized. In the free energy plot, we see that in case II and case III, for large ϵ the free energy curves approach linear with slope 1, reflecting that in this regime

[10]Indeed $f \sim 1$ near the equilibrium separation in case II and case III, $\partial f/\partial L \simeq 0$ in case IV, and in the quenched case $f \propto \epsilon$ with a logarithmic dependence when $l \simeq 1$.

most molecules are bound ($f \approx 1$); in the both-open system, the free energy has an exponential increase due to the incoming molecules from the reservoirs.

On the other hand the quenched case is essentially different. From above we have the estimate that $f \leq \phi\epsilon/k_{\rm B}T$, therefore $f \ll 1$ for the range of ϵ we choose. Naive estimate for l_0 gives $l_0 \sim f^{-1/4} \sim \epsilon^{-1/4} > 1$, which would be true only if f is independent of l. Even though the latter assumption does not hold in this regime, the qualitative trends still hold: we indeed observe that l_0 is bigger than in the annealed cases and decreases as ϵ increases.

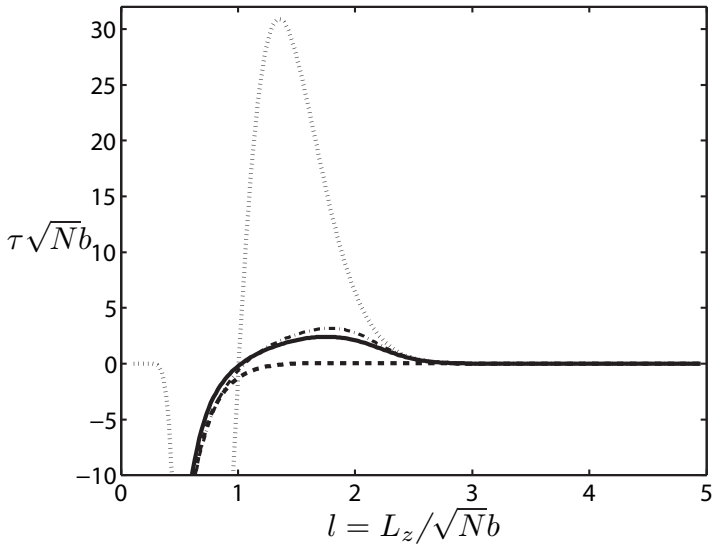

Figure 4.9: The force-extension curve for case I (dash line), II (solid line), III (dash-dot line), and IV (dot line). The binding energy is $\epsilon = 10k_{\rm B}T$ and the molecular densities are $\phi_{\rm L}^{(0)} = \phi_{\rm R}^{(0)} = 0.01$.

Finally from the interaction potential we calculate the equilibrium force defined as

$$\tau = \frac{\partial F}{\partial L_z}.$$

τ measures the force between the surfaces at a given surface separation in a quasi-equilibrium state. (We adopt the convention that τ is positive if the surfaces are attracting each other, i.e., one needs to exert force to pull the surfaces apart.) In Fig. 4.9 we plot $\tau\sqrt{N}b$ against the scaled surface separation l. If we neglect the weak dependence of ϵ on N, this is a scaling plot for $\tau\sqrt{N}b$ against l. One immediately sees that τ scales as $N^{-1/2}$ against the tether length, reflecting the finite range of binding attraction mediated by the polymer tether. The maximum in the force-extension curve corresponds to the critical pulling force above which the bond will be broken even in the quasi-equilibrium state (without fluctuations), which gives an upper bound of the bridging force (Moore

and Kuhl, 2006). From scaling arguments we would expect

$$\tau_{\rm c} \sim \frac{f\beta\epsilon}{l_1 - l_0} \sim f\left(\frac{\epsilon}{k_{\rm B}T}\right)^{1/2} N^{-1/2}.$$

For tether length $\sqrt{N}b \sim 3$nm and $\rho \sim 10^{-1}\text{nm}^{-2}$, $1k_{\rm B}T$ in Fig. 4.9 corresponds to a force per unit area 3.7 N/m^2. Therefore the critical stresses in different cases are 2N/m^2 (case I), 15N/m^2 (case II, III), and 100N/m^2 (case IV). The values are comparable to the results reported by Moore and Kuhl (2006), but larger than their values which are around $4\text{N}/m^2$. However, the polymer tether is significantly stretched in the experiments by Moore and Kuhl (2006) therefore the Gaussian chain approximation is invalid. In this strong stretching regime, the critical tension is approximately

$$\tau_{\rm c} \sim \frac{f\epsilon/k_{\rm B}T}{l_1 - l_0} \sim f\left(\frac{\epsilon}{k_{\rm B}T}\right) N^{-1}.$$

In summary, the interactions between surfaces due to ligands and receptors include the generic repulsion due to confinement and the specific attraction due to binding. The magnitude of the binding attraction is determined by the microscopic binding affinity, the tether lengths, and the molecular densities, through an effective binding constant and the scaled molecular densities. The net effect of binding attraction and confinement repulsion results in a free energy minimum at a surface separation comparable to the ideal size of a tethered bridge.

When one or both species are connected to a reservoir, molecules can be attracted into or pushed out of the system according to the interaction potential. Qualitatively different is the case when molecules are immobile. The free energy cost due to lateral stretching makes binding much less probable, resulting in a binding fraction considerably less than unity.

We further notice that in all these cases, the onset of binding (where the binding fraction starts to increase considerably) appears to be identical, reflecting the binding energy ϵ as a universal measure of binding strength; while the equilibrium bound state, which is dependent on the saturated density of bound molecules, differs in the various scenarios due to entropic effects (diffusion of molecules). The dependences of the equilibrium separation and the minimum free energy can be qualitatively explained using the scaling relations.

Since our results are based on equilibrium analysis but real systems or processes are usually non-equilibrium in nature, it is natural to ask in what situations these conclusions hold. Let's take the surface force measurement (Wong et al., 1997; Jeppesen et al., 2001) as an example. Here we observe three physical time scales, corresponding to the binding reaction ($\tau_{\rm r}$), the diffusion of the polymer tether (or the ligand/receptor group) in solution ($\tau_{\rm p}$), and the trans-membrane diffusion of polymers ($\tau_{\rm D}$). In addition there is the time scale corresponding to the relative speed at which surfaces are approaching or departing from each other (τ). Moore and Kuhl (2006) found that the polymer

diffusion time $\tau_{\rm p}$ (Zimm time) is roughly 1μs, and the binding reaction time $\tau_{\rm r}$ is typically several nanoseconds. The diffusivity of the protein across the membrane was quoted in Dustin et al. (1996) and Cuvelier et al. (2004) to be $10^{-8} \sim 10^{-9}{\rm cm}^2/{\rm s}$, which gives a time scale of $\tau_{\rm D} \sim (\rho D)^{-1} \sim 1$ms for the rearrangement of molecular distributions. Therefore we have

$$\tau_{\rm D} \gg \tau_{\rm p} \gg \tau_{\rm r}.$$

Generally $\tau \gg \tau_{\rm r}$, and it is always valid to treat the binding reaction as an equilibrium. If the surfaces approach very fast such that $\tau < \tau_{\rm p}$, then the diffusion of the polymer tether is relevant and this is the scenario analyzed by Moreira et al. (2003) and Moreira and Marques (2004) using reaction-diffusion theory. If the surfaces approach slow enough such that $\tau > \tau_{\rm D}$, then the system is essentially governed by the equilibrium thermodynamics and all our results should hold; if $\tau_{\rm D} > \tau > \tau_{\rm p}$, the system is in the quenched scenario as the diffusion of the molecules across the membrane is too slow to be treated as annealed.

Moreira et al. (2003), Moreira and Marques (2004), and Moore and Kuhl (2006) discussed the relevance of the approaching speed to the interacting force between the surfaces and the dependence of the fraction of bonds on the surface separation. For the dependence of the onset of binding (their "binding range") on the binding affinity, they found the same result as ours, $l_1 \propto \sqrt{\epsilon/k_{\rm B}T}$, which sets an upper bound in the dynamic measurements where surfaces approach at a finite speed; for the dependence on the tether length, our result suggests $l_1 \sim \sqrt{\epsilon/k_{\rm B}T}N^{\nu}b$, which agrees with their experimental results for long tethers[11]; for short tethers the finite extensibility of the tether should change the scaling dependence. The breaking of the bond is more subtle and is best put in a dynamic context (Evans and Ritchie, 1999; Sain and Wortis, 2004). But as discussed by Moore and Kuhl (2006), the equilibrium force gives an upper bound on the bridging force or the breaking force as long as the approaching or separating speed is not faster than the relaxation of the polymer segments. And our prediction that $\tau \sim \epsilon^{1/2}/N^{\nu}$ should hold for long chains in this regime. Thermal fluctuations will even lower the threshold for breaking the bond, as was considered by Sain and Wortis (2004).

The distinct time scales of motion result in different physical scenarios. For example, the diffusion of ligand and/or receptor groups is governed by the diffusion of the polymer tether as well as the diffusion of the anchoring end in the membrane. But the diffusion in the bilayer is much slower compared to the diffusion of polymer segments in the solution, therefore tethered ligands and receptors can locate their counterparts more easily and result in faster adhesion dynamics compared with the adhesion without tether, as was observed by Cuvelier and Nassoy (2004). In addition the polymer tether increases the range of binding, which admits larger membrane deformations compared with the case of molecular binding: such membrane fluctuations lower the energy barrier

[11] Moreira et al. (2003) and Moreira and Marques (2004) did not do a scaling plot.

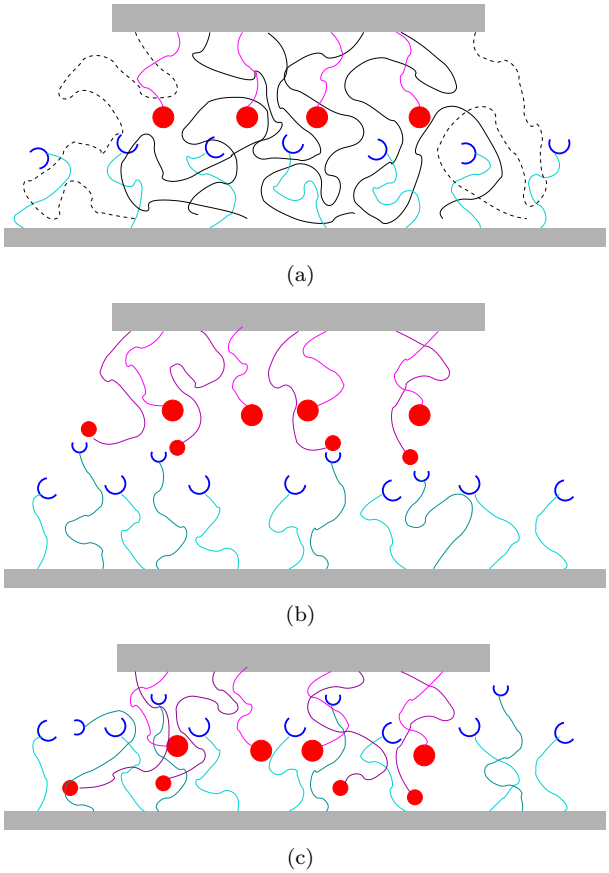

Figure 4.10: Schematic views of the models to be discussed in Section 4.3.3.1 (a), Section 4.3.3.2 (b), and Section 4.3.3.3(c). When molecules with different lengths are present, we usually scale the densities by the length of the (shorter) tethered ligand-receptor bridge, and refer to the molecular densities of other species relative to the density of ligands or receptors.

of adhesion and stabilize the bound state. These two effects qualitatively explain the experimental findings by Cuvelier and Nassoy (2004), although quantitative treatments require an analysis of the adhesion dynamics, which is beyond the scope of our current paper.

4.3.3 Composite interaction potential from specific binding and non-specific interactions

In previous subsections we discuss the interactions between surfaces mediated by polymer-tethered ligand-receptor binding. Real biological processes, however, usually involve many different types of ligand-receptor interactions, with different binding affinities or tether lengths. (See Springer (1990) for a snapshot of different proteins involved in immunological responses.) Even in a simple cell adhesion, the polysaccharide layer on the cell surface introduces additional repulsion between the cell surface and the external surface. This repulsive layer effectively prevents non-specific and preserves specific adhesion.

Here we study the overall interaction potential between the surfaces mediated by several specific and non-specific interactions. We neglect non-specific intra- and intermolecular interactions, such as the excluded volume, and focus on the features of specific interactions and generic repulsion. From these examples we try to illustrate the different features associated with each interacting species and provide some general principles for the design and control of surface interactions.

4.3.3.1 Cell adhesion revisited

Bell and co-workers (Bell, 1978; Bell et al., 1984; Torney et al., 1986) first proposed that cell adhesion is a net result of specific ligand-receptor binding and non-specific steric repulsion due to repelling molecules on the cell surface. Here we re-examine this model and study the dependence of the interaction potential on measurable and controllable molecular parameters, which can guide bioengineering design of artificial surfaces that can trigger cell adhesion. Specifically we treat the binding molecules as polymer-tethered ligands and receptors and the repelling polymers as linear Gaussian chains confined between surfaces [12]. The model is schematically shown in Fig. 4.10(a).

Figure 4.11 shows the composite interaction potential due to ligand-receptor binding and steric repellers. In Fig. 4.11(a) the system belongs to case III (open-closed system) and we plot the cases with mobile repellers (dash line) and immobile repellers (thick solid line). The interaction potential due to ligand-receptor interactions alone is shown for comparison (thin solid line).

The repeller polymer has length $N_{\rm r} = 16(N_{\rm L} + N_{\rm R})$, hence the repulsion is present at

$$L_z \sim \sqrt{N_{\rm r}}b = 4\sqrt{N_{\rm L} + N_{\rm R}}b \gtrsim \sqrt{\beta\epsilon}\sqrt{N_{\rm L} + N_{\rm R}}b,$$

which is slightly larger than the separation at the onset of binding. When repellers are mobile, the repulsive potential flattens off at small separation, implying that they are squeezed out (or "redistributed" in Bell's terminology). This introduces a modest barrier (osmotic pressure) that is proportional to the density of repellers; the length of repellers only affects the range of repulsion, not the barrier height. When repellers are immobile, the short-range repulsion scales as $N_{\rm r}b^2/L_z^2$ and presents a strong repulsion. Accordingly the equilibrium bound state is shifted towards larger surface separations with shallower free energy minimum, due to the strong repulsion at small surface separations.

In Fig. 4.11(b), we examine the case when both receptors and ligands are connected to a reservoir with densities $\phi^{(0)} = 0.005$ and with immobile repeller polymers at different densities. Contrary to the case of receptors/ligands with fixed densities, the equilibrium separation is shifted very little, although the free energy minimum becomes shallower if not vanishing. This suggests a way to adjust

[12] Simple scaling tells us that the short-range repulsion due to confinement of Gaussian chains scales as $\sim Nb^2/L_z^2$, Nb^2 being the mean square end-to-end distance of the polymer and L_z the spatial confinement size. In the Bell model, the repulsion is assumed to scale as $\propto (L_z)^{-1}$; this would correspond to stretched polymers in the brush regime. Extension to this scenario can be straightforwardly implemented via self-consistent calculation.

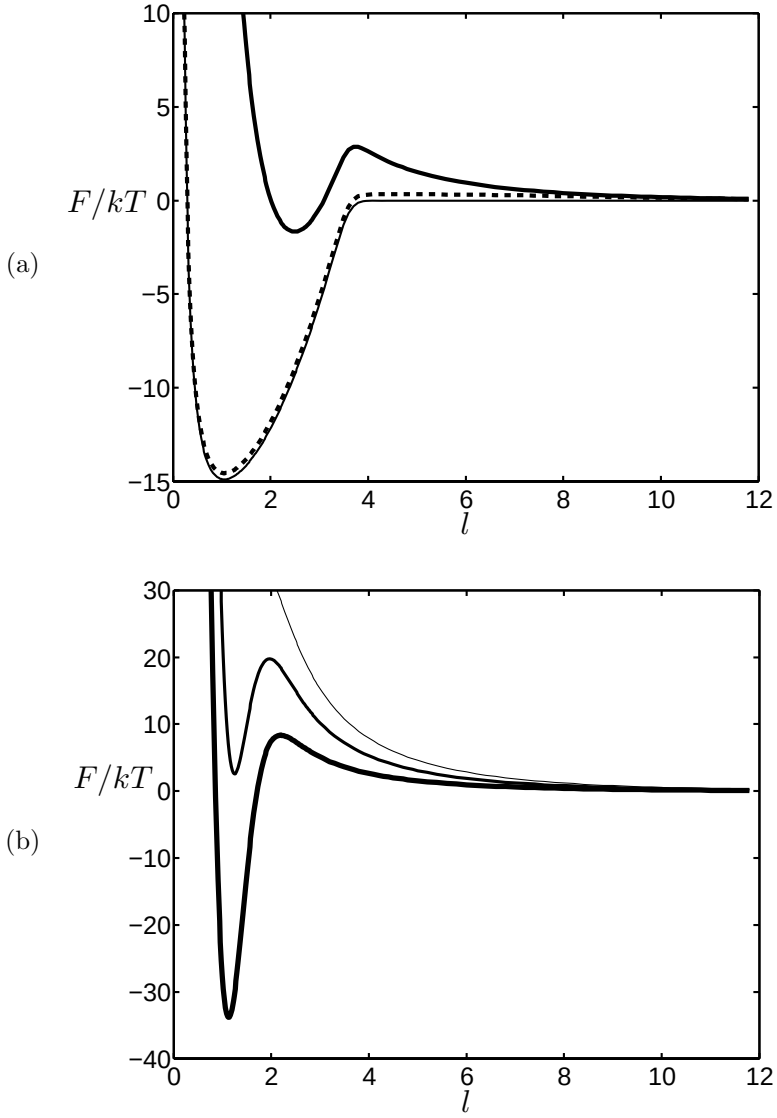

Figure 4.11: The interaction between surfaces mediated by ligand-receptor binding and repulsive polymers. The ligand-receptor binding has a binding energy $\epsilon = 15k_{\rm B}T$. The length of repelling polymers is $N_{\rm r} = 16(N_{\rm L}+N_{\rm R})$. In (a) the densities of ligands and receptors are $\rho^{(0)}(N_{\rm L}+N_{\rm R})b^2 = 1$ and the repeller density is $\rho_{\rm r} = \rho^{(0)}/3$. The dash line is for mobile repellers and the thick solid line for immobile repellers; the thin line is for the bare ligand-receptor system without repellers. (b) Receptors and ligands are both in open system (case IV) with reservoir densities $\rho^{(0)}(N_{\rm L}+N_{\rm R})b^2 = 0.005$, the binding energy is the same as in (a); from above the densities of repelling polymers are: $\rho_{\rm r} = \rho^{(0)}$ (thinnest), $\rho_{\rm r} = 2\rho^{(0)}/3$ (moderate), and $\rho_{\rm r} = \rho^{(0)}/3$ (thick).

the depth of the free energy of the bound state independent of its location, as compared to the case in Fig. 4.11(a) where the two are correlated.

Recently Bruinsma et al. (2000) studied the adhesion between a large versicle and a lipid bilayer when both receptors and repellers are present. They observed that tightly bound regions with higher densities of receptors coexist with loosely bound states with lower densities, and receptors

slowly aggregate to the tightly bound regions (focal adhesion zone). This coexistence was argued to result from a double-well inter-membrane potential separated by a barrier induced by the repeller molecules. The authors further pointed out that the repellers are better characterized as mobile with a given chemical potential so that they can be pushed out in the tightly bound regions.

In our model we do not account for the long-range physical interactions or membrane deformations, which result in the loosely bound minimum described in the Bruinsma paper. Otherwise our analysis qualitatively agrees with their observations. In addition we point out that since the growth of the contact area is slow, initially the adhesion zone should be viewed as an open system of receptors with the loosely bound part serving as the reservoir. This was also observed by Dustin et al. (1996). The attraction inside the focal contact is significantly higher than that predicted from the overall density on the surface, which can overcome the barrier due to immobile repellers; such a process would be impossible if the binding molecules were uniformly distributed as in a closed ensemble.

Finally we point out that due to the barrier between the bound and the unbound state, even in flat geometries the adhesion process should be a first-order transition (Bruinsma and Sackmann, 2002; Weikl et al., 2002). Therefore the presence of a considerable barrier is adequate to prevent non-specific adhesion even though the bound minimum still exists. In this case the growth of the adhesion contact is through nucleation, which is most likely mediated by membrane fluctuations. We will study this interplay between membrane fluctuations and ligand-receptor interactions in Chapter 5.

4.3.3.2 Bidisperse ligand-receptor binding

Introducing long repelling polymers can generate a barrier from the unbound to the bound state, thus preventing unwanted binding or adhesion between the surfaces. If, instead of purely repelling polymers, we introduce longer-tethered ligands and receptors, then these molecules act as a "barrier" to the shorter-tethered binding, but on the other hand generate another minimum at a larger surface separation. Properly adjusting the binding affinities and tether lengths of these two ligand/receptor pairs gives us extra freedom in controlling the strength and range of the attraction between the surfaces.

Here we consider a system with two ligand-receptor pairs with different tether lengths and affinities, as schematically represented in Fig. 4.10(b). The interaction potentials are shown in Fig. 4.12. The shorter-tethered ligand/receptor pair has a larger binding energy $\epsilon = 15k_{\mathrm{B}}T$ and higher density $\phi_1^{(0)} = 1$, and we assume them to be an "open-closed" system to mimic cell-substrate interactions. The longer-tethered one has a smaller binding energy $\epsilon = 5k_{\mathrm{B}}T$ and smaller density $\rho_2^{(0)} = 0.5\rho_1^{(0)}$ (note that this is the molecular density instead of the scaled density ϕ) and we assume both of them to be in a closed system.

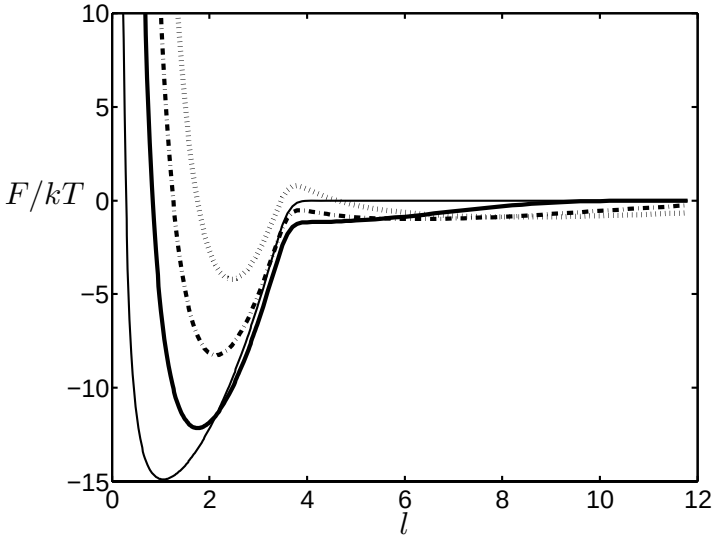

Figure 4.12: The interaction potential resulting from binary ligand-receptor interactions. Ligands and receptors have equal densities as their counterparts. The short-tethered ligand-receptor pairs have $\epsilon_1 = 15k_{\rm B}T$, and $\phi_1^{(0)} = 1$, and the system belongs to case III (open-closed). The thin line represents the interaction potential of this system alone. The long-tethered ligand-receptor pairs have weaker binding energy $\epsilon_2 = 5k_{\rm B}T$, with fixed densities (case II) $\rho_2^{(0)} = 0.5\rho_1^{(0)}$. Both ligand-receptor pairs have equal lengths for ligand and receptor tether. From above, the lengths of the longer tethers are: $N_2 = 64N_1$ (dot line), $N_2 = 36N_1$ (dash-dot line), and $N_2 = 16N_1$ (thick solid line).

Since the long-tethered molecules introduce a barrier to the short-tethered binding and generate a new free energy minimum at larger separation, the superimposed interaction potential should take a double-well shape. In Fig. 4.12 the dot line represents the case with tether ratio $N_2/N_1 = 64$, the dash-dot line for $N_2/N_1 = 36$, and the thick solid line for $N_2/N_1 = 16$; the thin solid line is for the system with short-tethered ligands and receptors only, the same as in Fig. 4.11(a). For the range of tether lengths we studied, we see that the minimum due to the short-tethered binding is shifted to larger separations with higher free energies, similar to Fig. 4.11(a).

When the length of the long-tethered bridge is much larger than that of the short-tethered one (dot line), we observe two minima separated by a positive barrier. If the long tether is of intermediate size (dash-dot line), we still observe two separate minima, but the barrier between them is small and negative; for comparable tether lengths (thick solid line), the two minima merge with a larger range of attraction. These results demonstrate that by adjusting the relative length ratio one can qualitatively control the shape of the interaction potential from single well to double well.

Understanding the interactions due to binary ligand-receptor binding is both relevant to surface engineering and to our understanding of biological systems. In a colloidal suspension with particles interacting via a double-well potential, we expect structures with competing length scales of ordering

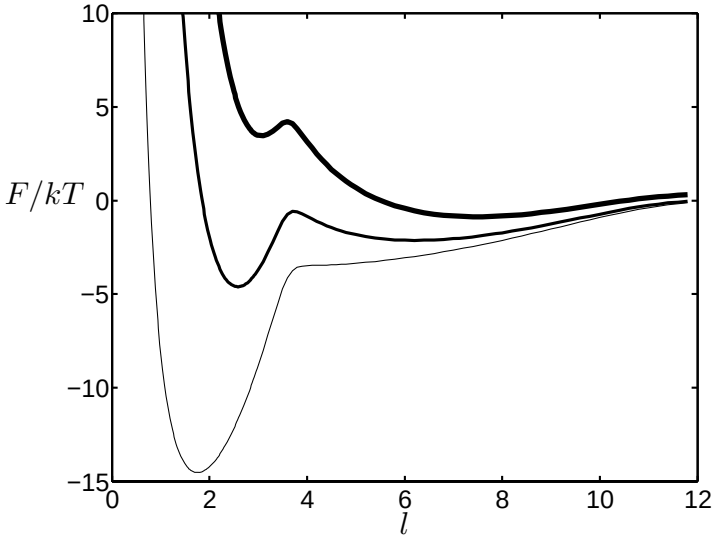

Figure 4.13: Interaction between surfaces with two different ligand-receptor interactions and repelling polymers. For short-tethered ligands/receptors we have $\epsilon_1 = 15k_{\rm B}T$, and $\phi_1^{(0)} = 1$; for the long-tethered ligands/receptors we have $\epsilon_2 = 10k_{\rm B}T$, $\rho_2^{(0)} = 0.5\rho_1^{(0)}$, and $N_2 = 16N_1$. Ligand and receptor tether lengths are equal for both types. And the short-tethered binding is assumed to belong to case III (open-closed) and the long one to case II (both closed). The lengths of the immobile repelling polymers are $N_{\rm r} = 36N_1$ (thickest line) and $N_{\rm r} = 16N_1$ (intermediate) with density $\rho_{\rm r} = \rho_1^{(0)}/3$.

with complicated symmetries, as well as colloidal gels with local but no long-range order[13]. On the other hand, it is known that in the rolling of leukocyte cells (Lawrence and Springer, 1991; Springer, 1994), the longer but weaker selectin ligands mediate rolling of the cells, while the shorter but stronger integrin receptors result in the final strong adhesion; the interplay between longer-tethered ligands and shorter-tethered ligands is key to the successful immunological response (Qi et al., 2001). For stable rolling, the double-well shape interaction potential might be crucial.

4.3.3.3 Attempt at a synthesis

From the above examples we have seen two ways to adjust the interaction potential between surfaces: (1) introduce a barrier from the unbound to the bound state by adding longer repelling polymers; (2) shift the equilibrium separation and the minimum free energy and allow different minima to appear by combining ligand-receptor pairs of different lengths.

Let's summarize the main results in these two cases. To introduce a barrier to the bound state, mobile repellers introduce a less noticeable barrier and smaller shift to the equilibrium separation compared with immobile repellers; with immobile repellers increasing the density or the chain length of the repeller molecules can both increase the barrier height, but the latter will also result in a larger range of repulsion. When a different type of ligand/receptor pairs with longer tethers is introduced,

[13]See Hiddessen et al. (2000) for some examples using single ligand-receptor pairs.

depending on the tether lengths, the system can show two free energy minima separated by a large barrier (large tether-length difference), two minima separated by a small barrier (intermediate tether-length difference), or one minimum only (comparable tether lengths). Adjusting the density of each type of ligand/receptor molecules allows us to control the relative stability of the minima due to each ligand-receptor pair.

Combining these two methods allows us to control the subtle features of the interaction potential. Here we just give one example to illustrate how the relative stability of the minima in a bidisperse ligand-receptor system can be controlled by introducing repellers of different lengths. In Fig. 4.13 the thin line represents the system with bidisperse ligand/receptor molecules with parameters: $\epsilon_1 = 15k_{\rm B}T$, $\phi_1^{(0)} = 1$, and $\epsilon_2 = 10k_{\rm B}T$, $N_2 = 16N_1$, $\rho_2^{(0)} = 0.5\rho_1^{(0)}$. Comparing Fig. 4.13 with Fig. 4.12, we see that although the binding energy for the longer-tethered ligand/receptor molecules is larger, the qualitative features are identical, hence changing the binding energy has little effect on the shape of the interaction potential. However, by introducing immobile repeller molecules with a fixed density $\rho_{\rm r} = \rho_1^{(0)}/3$ but different lengths, we can qualitatively control the interaction potential. In both cases we see two separate minima. For long repellers ($N_{\rm r} = 36N_1$, thickest line) the stable one is at the larger separation, corresponding to the longer-tethered binding, and the repellers generate a barrier to the bound state. In the case of short repellers ($N_{\rm r} = 16N_1$) the stable bound state is at the smaller separation and there is no barrier from unbound to the longer-tethered bound state.

Clearly one can introduce more species into the system to adjust the individual features independently. Because of the specificity of ligand-receptor binding, each type of ligand-receptor binding is independent of others, and the total interaction potential is the superposition of all ligand-receptor pairs, which provides a diverse and powerful way to engineer surface interactions.

4.4 Conclusion

We have studied a continuum microscopic model for polymer-tethered ligand-receptor interactions between surfaces and analyzed the thermodynamics of interactions between the surfaces, which essentially consist of a repulsion due to the confinement of polymers at small surface separations, and an attractive binding at intermediate range of separations mediated by the polymer tether. The generic short-range repulsion due to confinement can be calculated or estimated from scaling analysis for a given chain model. For the tethered binding we find an effective binding constant that relates the density of bound pairs to those of ligands and receptors.

The binding constant has contributions from a microscopic binding affinity between the ligand and the receptor group, which is independent of the surface separation or tether lengths, and a tether stretching energy, which reflects the conformation change of the polymer tethers due to binding. At small surface separations, the 2D binding constant is independent of the tether length, and can

be related to the 3D binding constant by $K^{2D} = K^{3D}/\text{surface separation}$, but at large surface separations the stretching energy is important. The attractive binding and the repulsion due to confinement result in an equilibrium separation between the surfaces corresponding to the minimum of the total interaction free energy.

For the overall interactions between surfaces, we study the different scenarios when binding molecules have different mobilities. Specifically ligands and receptors can be immobile, mobile with a fixed density, or mobile with a fixed chemical potential. These different scenarios correspond to binding between objects with different geometries or different molecular embeddings. Binding is least probable in the case when both species are immobile. On the other hand, in the cases with open ensembles, molecules are attracted into or pushed out of the system due to the net interaction, resulting in a lower free energy. In particular, for the case with ligands in a closed system and receptors in an open system, the maximum density of bound ligand-receptor pairs is determined by the fixed density of ligands, and is insensitive to the reservoir density, as is observed in experiments.

We illustrate our calculations using an ideal-Gaussian-chain model. Simple scaling arguments yield that the onset of binding (adhesion range) scales as $L_z^1 \sim \sqrt{\epsilon/k_B T}\sqrt{N}b$, and the equilibrium separation scales as $L_z^0 \sim \sqrt{N}b$. These results agree well with the exact solutions. We also infer that the quasi-equilibrium critical tension as obtained from the equilibrium force-extension curve should scale as $N^{-1/2}$ for the Gaussian tether. These scaling dependences should also hold for non-Gaussian chain models by replacing the $N^{1/2}$ factor with the characteristic size of the polymer chain (N^{ν}).

Finally we demonstrate that by combining different types of ligand-receptor interactions and non-specific repeller molecules, one can achieve precise control over the interaction potential between surfaces. Specific examples include introducing a barrier between the unbound and the bound state and introducing multiple minima and controlling the range and magnitude of each minimum. These results suggest possible strategies for bioengineering design with better specificity and for a diverse control of surface interactions using specific interactions.